



Overview of the
Manitou
Experimental Forest
Observatory

J. Ortega et al.

This discussion paper is/has been under review for the journal Atmospheric Chemistry and Physics (ACP). Please refer to the corresponding final paper in ACP if available.

Overview of the Manitou Experimental Forest Observatory: site description and selected science results from 2008–2013

J. Ortega¹, A. Turnipseed¹, A. B. Guenther^{1,a}, T. G. Karl^{1,b}, D. A. Day², D. Gochis¹, J. A. Huffman^{3,4}, A. J. Prenni⁵, E. J. T. Levin⁵, S. M. Kreidenweis⁵, P. J. DeMott⁵, Y. Tobo⁵, E. G. Patton¹, A. Hodzic¹, Y. Cui⁶, P. C. Harley^{1,c}, R. H. Hornbrook¹, E. C. Apel¹, R. K. Monson⁷, A. S. D. Eller^{8,d}, J. P. Greenberg¹, M. Barth¹, P. Campuzano-Jost², B. B. Palm², J. L. Jimenez², A. C. Aiken⁹, M. K. Dubey⁹, C. Geron¹⁰, J. Offenberg¹¹, M. G. Ryan^{12,13}, P. J. Forwalt¹³, S. C. Pryor¹⁴, F. N. Keutsch¹⁵, J. P. DiGangi^{15,e}, A. W. H. Chan^{16,f}, A. H. Goldstein^{16,17}, G. M. Wolfe^{18,19}, S. Kim^{1,g}, L. Kaser^{20,h}, R. Schnitzhofer²⁰, A. Hansel²⁰, C. A. Cantrell^{1,i}, R. L. Mauldin III^{1,i}, and J. N. Smith¹

¹National Center for Atmospheric Research, P.O. Box 3000, Boulder, CO 80307, USA

²Department of Chemistry and Biochemistry and Cooperative Institute for Research in the Environmental Sciences (CIRES), University of Colorado, Boulder, CO 80309, USA

³Max Planck Institute for Chemistry, P.O. Box 3060, 55020, Mainz, Germany

⁴University of Denver, Department of Chemistry & Biochemistry, Denver, CO 80208, USA

⁵Department of Atmospheric Science, Colorado State University, Fort Collins, CO 80523, USA

Title Page

Abstract

Introduction

Conclusions

References

Tables

Figures



Back

Close

Full Screen / Esc

Printer-friendly Version

Interactive Discussion



^cnow at: Department of Plant Physiology, Estonian University of Life Sciences, Tartu 51014, Estonia

^dnow at: Department of Biological Sciences, Macquarie University, Sydney, NSW, 2109, Australia

^enow at: Department of Civil and Environmental Engineering, Princeton University, Princeton, NJ 08544, USA

^fnow at: Department of Chemical Engineering and Applied Chemistry, University of Toronto, Canada

^gnow at: Department of Earth System Science, University of California, Irvine, Irvine, CA 92697, USA

^hnow at: National Center for Atmospheric Research, P.O. Box 3000, Boulder, CO 80307, USA

ⁱnow at: Department of Atmospheric and Oceanic Sciences, University of Colorado, Boulder, CO 80309, USA

Received: 23 November 2013 – Accepted: 18 December 2013 – Published: 20 January 2014

Correspondence to: J. N. Smith (jimsmith@ucar.edu)

Published by Copernicus Publications on behalf of the European Geosciences Union.

Overview of the
Manitou
Experimental Forest
Observatory

J. Ortega et al.

Title Page

Abstract

Introduction

Conclusions

References

Tables

Figures

◀

▶

◀

▶

Back

Close

Full Screen / Esc

Printer-friendly Version

Interactive Discussion

Abstract

The Bio-hydro-atmosphere interactions of Energy, Aerosols, Carbon, H₂O, Organics & Nitrogen (BEACHON) project seeks to understand the feedbacks and inter-relationships between hydrology, biogenic emissions, carbon assimilation, aerosol properties, clouds and associated feedbacks within water-limited ecosystems. The Manitou Experimental Forest Observatory (MEFO) was established in 2008 by the National Center for Atmospheric Research to address many of the BEACHON research objectives, and it now provides a fixed field site with significant infrastructure. MEFO is a mountainous, semi-arid ponderosa pine-dominated forest site that is normally dominated by clean continental air, but is periodically influenced by anthropogenic sources from Colorado Front Range cities. This article summarizes the past and ongoing research activities at the site, and highlights some of the significant findings that have resulted from these measurements. These activities include:

- soil property measurements,
- hydrological studies,
- measurements of high-frequency turbulence parameters,
- eddy covariance flux measurements of water, energy, aerosols and carbon dioxide through the canopy,
- biogenic and anthropogenic volatile organic compound emissions and their influence on regional atmospheric chemistry,
- aerosol number and mass distributions,
- chemical speciation of aerosol particles,
- characterization of ice and cloud condensation nuclei,
- trace gas measurements, and

Overview of the Manitou Experimental Forest Observatory

J. Ortega et al.

Title Page

Abstract

Introduction

Conclusions

References

Tables

Figures



Back

Close

Full Screen / Esc

Printer-friendly Version

Interactive Discussion



- model simulations using coupled chemistry and meteorology.

In addition to various long-term continuous measurement, three focused measurement campaigns with state-of-the-art instrumentation have taken place since the site was established, and two of these are the subjects of this special issue: BEACHON-ROCS (Rocky Mountain Organic Carbon Study, 2010) and BEACHON-RoMBAS (Rocky Mountain Biogenic Aerosol Study, 2011).

1 Introduction

1.1 Motivation

Development of Earth-System models is driven by the need to improve the predictability of atmospheric chemical and physical processes over time scales ranging from minutes to decades. Accurate model predictions are critically contingent on process-level understanding and detailed numerical descriptions of the coupling between water, energy and biogeochemical cycles across temporal and spatial scales (Denman et al., 2007; Alo and Wang, 2008; Heald et al., 2009). A number of studies have discussed some of these processes and associated feedbacks (e.g. Barth et al., 2005; Carslaw et al., 2010; Mahowald et al., 2011), but more detailed observations and coordinated modeling efforts are required for improved representation in Earth-System models.

The Bio-hydro-atmosphere interactions of Energy, Aerosols, Carbon, H₂O, Organics & Nitrogen (BEACHON) project was initiated by the National Center for Atmospheric Research (NCAR) as well as collaborators from the University of Colorado and Colorado State University to investigate ecosystem-atmosphere exchange of trace gases and aerosols and their potential feedbacks between biogeochemical and water cycles. BEACHON is now an ongoing component of atmospheric research sponsored by the National Science Foundation. This interdisciplinary research program integrates local and regional model simulations with remote sensing, regional network observations,

Overview of the Manitou Experimental Forest Observatory

J. Ortega et al.

Title Page

Abstract

Introduction

Conclusions

References

Tables

Figures

⏪

⏩

◀

▶

Back

Close

Full Screen / Esc

Printer-friendly Version

Interactive Discussion



the atmospheric chemistry measured at the site through changes in gas- and aerosol-phase emissions from nearby fire-scarred vegetation and soil. Wildfires are ubiquitous in the semi-arid forested American West, of which this area can be considered representative.

5 The Manitou Experimental Forest's elevation ranges from 2280 to 2840 m.a.s.l., and vegetation is primarily composed of forests of ponderosa pine, Douglas-fir, mixed conifer and aspen. The forest stands surrounding the observatory are relatively young, uneven-aged stands dominated by ponderosa pine (Sect. 1.3). Leaf area index (LAI) measurements from representative trees resulted in a value of 3.0. The fractional cover-
10 erage of the ponderosa pine surrounding the observatory is 0.38 resulting in an effective leaf area index for the site of 1.14 and average canopy height of 18.5 m. In 2009, core samples from a survey of 38 representative ponderosa pine showed that the median tree age was 49.5 yr (with average, minimum and maximum ages of 62.5, 27, and 201 yr respectively). Soils are mostly derived from weathered granite, are poorly
15 developed, and prone to erosion. The National Weather Service has been monitoring precipitation at MEF since 1940 (Station Woodland Park 8 NNW, Coop ID: 059210), and US Forest Service staff have been collecting meteorological data including air and soil temperature, precipitation, and wind speed since 1998. These data indicate that the climate is cool (mean temperature is 19 °C in July and -2 °C in January) and dry with an
20 average annual precipitation for 2010–2013 of 430.5 mm (16.94 inches). Approximately 50 % of the precipitation falls as rain during the summer season (June–September) primarily during afternoon thunderstorms characterized by brief but intense periods of rainfall and lightning. Winter snowfall is typically light, and a persistent snowpack rarely develops.

25 Numerous studies have been conducted here by researchers from a wide range of federal agencies, academic institutions, and non-governmental organizations. Early research focused on range management, including re-vegetation of abandoned fields, grazing management in native and seeded pastures, watershed management in gully control, stream sedimentation, surface runoff, bacterial pollution, and infiltration (Gary

Overview of the Manitou Experimental Forest Observatory

J. Ortega et al.

Title Page

Abstract

Introduction

Conclusions

References

Tables

Figures

⏪

⏩

◀

▶

Back

Close

Full Screen / Esc

Printer-friendly Version

Interactive Discussion

Kipp and Zonen CNR1 radiometer for measuring above-canopy incoming and outgoing shortwave and longwave radiation. Instrumentation on the other five levels include:

- Campbell-Scientific CSAT3 sonic anemometers to record the three orthogonal wind velocity components and temperature fluctuations;
- NCAR-Vaisala aspirated hygrothermometers to measure absolute temperature and relative humidity;
- LI-COR open-path infrared gas analyzers to measure water vapor and carbon dioxide.

The instruments on the micrometeorology tower operated nearly continuously from July 2009 until July 2012 when they were removed as a precaution due the proximity of the Waldo Canyon Fire. This multi-season dataset is being used to:

- quantify the importance of canopy-induced modifications to turbulence in predicting whole-ecosystem exchange in regional and global climate models,
- partition water fluxes into transpiration and evaporation components, and
- investigate impacts of spatially heterogeneous canopy distributions on evapotranspiration using additional information from the chemistry and understory towers.

The chemistry tower is a 28 m walk-up type tower that is equipped with meteorological sensors as well as a variety of flux and gradient concentration measurements for gasses and aerosols (Fig. 1d). The platform on each level is 1.78 m × 1.27 m and is suitable for heavier instruments that require more space, power and maintenance. It can also support gradient sampling systems, which can move vertically along the tower. This tower is equipped with 2-D and 3-D sonic anemometers, temperature, and radiation probes for continuous meteorological measurements and for calculating fluxes using the closed-path eddy covariance method. Other continuous gas-phase measurements from this tower include: CO, CO₂, H₂O vapor, NO, NO₂ and SO₂.

Overview of the
Manitou
Experimental Forest
Observatory

J. Ortega et al.

Title Page

Abstract

Introduction

Conclusions

References

Tables

Figures



Back

Close

Full Screen / Esc

Printer-friendly Version

Interactive Discussion



Overview of the Manitou Experimental Forest Observatory

J. Ortega et al.

Title Page

Abstract

Introduction

Conclusions

References

Tables

Figures

⏪

⏩

◀

▶

Back

Close

Full Screen / Esc

Printer-friendly Version

Interactive Discussion

vapor for a complete accounting of the site's water budget. The precipitation measurements augment the long-term records maintained by the USDA Forest Service mentioned in Sect. 1.2. A network of 11 tipping bucket rain gauges as well as an unshielded, weighing-type total precipitation gauge provide high time resolution, year-round precipitation measurements in a network distributed within the chemistry tower footprint in order to characterize the high spatial variability of precipitation. More details about these measurements are given in Table S1. The 2010–2013 annual accumulation of hourly precipitation is shown in Fig. 4a. These time series are bias-corrected merged data products between the site's sensors in order to cover periodic data gaps. The site's annual precipitation measurements for a given year are defined by an end date of 30 September of that year and a start date of 1 October in the preceding year. The patterns observed have been fairly consistent. Periodic precipitation episodes occur throughout the principal cool season of October through May followed by a brief dry season from late May through mid-June. This is followed by a summer period of rather intense precipitation episodes associated with the regional incursion of the North American Monsoon system. Finally there is an extended dry period starting in the late summer and extending into early autumn. The average annual accumulated precipitation for 2010–2013 was ~ 430.5 mm with a range of 392 mm (in 2012) to 513 mm (in 2010). It should be noted that 2012 was among the driest years on record for most of the state, and the total precipitation for 2013 was similarly low. The latter year began with very low winter and spring snow fall, and stayed much drier than average until heavy September rains finally increased the total accumulated precipitation to about the same level observed in 2012. During most years, approximately 50 % of the total precipitation occurs during June–September. The maximum observed hourly rainfall recorded at the site from 2009–2013 was 57.9 mm, which occurred on 4 August 2010. Other thunderstorms with high rain fall rates (up to 25 mm h^{-1}) are common during the summer monsoon.

Seasonally-transient snowpack is an important feature of the hydrologic cycle as the snowpack can provide a lasting water source to the site during the spring melt period

and can also insulate the soil from freezing temperatures. Snow depth measurements (Jenoptik, Inc. SHM30 laser snow depth sensor) began during the winter of 2010–2011. Persistent patchy or complete snowpack is limited to December, January and February. Periodic snowstorms may also input appreciable moisture during the months of October, November, March and April although the snowpack rarely persists for more than 7 days.

Soil moisture (Decagon EC-5 probes) and temperature (Campbell Scientific T107 thermistor) profiles extending from the near surface to approximately 1 m depth are made at 3 different sites within the micrometeorology tower's footprint. The merged annual cycle of soil moisture from all sites is shown in Fig. 4b, and the annual soil temperature cycle is shown in Fig. 4c. The soil moisture cycle exhibits some interesting and classic features of western landscape hydrology, especially the tendency for persistent dryness and pulsed recharge of near-surface moisture, particularly in the warm season. Deeper into the soil, the moisture variability is significantly damped and there is evidence of persistent soil moisture there, regardless of extended summer dry periods. This deeper layer of persistent wet soil helps sustain some of the total evaporative flux from the ponderosa pine ecosystem during the summer. There are extended periods of winter soil temperatures several degrees below 0°C, which extends to approximately 70 cm below the surface. These low soil temperatures indicate that significant amounts of soil water freeze (i.e., creates "soil frost") occasionally during the winter. The presence of soil frost is further evidenced by the sharp decline in recorded soil moisture values from December through late-February. Suppressed soil moisture values corresponding with sub-zero soil temperatures is a classic measurement artifact due to the significant change in soil dielectric permittivity as water undergoes phase change from liquid to ice and back again at the freezing point. This meltwater release and periodic melting of the transient snowpack impart additional water pulses to the site. As previously mentioned, MEFO typically experiences an early summer dry period before the onset of the monsoon rains, which is highly correlated with increased CO₂ and BVOC fluxes. The semi-arid climate creates very low mid-day stomatal conductance in pon-

Overview of the Manitou Experimental Forest Observatory

J. Ortega et al.

Title Page

Abstract

Introduction

Conclusions

References

Tables

Figures

⏪

⏩

◀

▶

Back

Close

Full Screen / Esc

Printer-friendly Version

Interactive Discussion



derosa pine during the early- and late-summer dry periods, which protects the trees from water stress. These fluxes and stomatal conductance both increase substantially during the monsoon rains.

2.2 Water manipulation effects on ponderosa pine

5 Projected water limitations and higher temperatures are expected to put additional climate-induced physiological stresses on semi-arid forest ecosystems (Allen et al., 2010). To test hypotheses related to future climates, manipulation experiments must be carefully designed to ensure that data are representative of larger ecosystems responses (Beier et al., 2012). With these considerations in mind, another study at
10 MEFO during 2010–2011 was designed to quantify the effect of different water treatments on the photosynthesis and respiration rates as well as BVOC emissions from mature trees (at least 10 m in height). Up to 50% of the incoming precipitation (snow and rain) was systematically diverted from the root zones (10 m × 10 m area) around targeted trees using an array of troughs (see Fig. 1c). The intercepted water was collected
15 into barrels and then added to nearby trees resulting in a water continuum delivered to the various trees from 0.5 to 1.5 times the total precipitation such that the total amount of water delivered to the entire plot remained constant. Physiological parameters (e.g. sapflow, photosynthesis, and BVOC emissions) were measured on all trees within the experimental plot. Similar to the speciation seen in ambient air, branch-level measurements showed that the BVOCs emitted in the highest concentrations were methanol,
20 2-methyl-3-buten-2-ol, and monoterpenes. Initial observations showed that seasonality in plant physiological processes and weather dynamics interact to produce complex controls over climate-dependent emissions of these compounds with a strong dependence on soil moisture and precipitation. If the climate in this region shifts to a drier
25 summer regime, total BVOCs emitted from needles of this forest are likely to decrease, which will have implications for modeling both gas- and liquid-phase regional chemistry. Studies such as this exemplify the interdisciplinary research questions addressed by

Overview of the Manitou Experimental Forest Observatory

J. Ortega et al.

Title Page

Abstract

Introduction

Conclusions

References

Tables

Figures

⏪

⏩

◀

▶

Back

Close

Full Screen / Esc

Printer-friendly Version

Interactive Discussion



the BEACHON project, and are necessary to address the ecological system processes for inclusion into Earth-System models as discussed in Sect. 1.1.

3 Volatile organic compounds, oxidants and aerosol properties

3.1 Volatile organic compound observations

5 Volatile organic compounds (VOCs) at MEFO are a mixture of biogenic and anthropogenic compounds. The summertime VOC signals are dominated by biogenic emissions, primarily methanol, ethanol, acetone, monoterpenes ($C_{10}H_{16}$, abbreviated by MT) and 2-methyl-3-buten-2-ol ($C_5H_{10}O$, abbreviated by 232-MBO or MBO). Isoprene (C_5H_8) is also observed during summer, but to a much lesser extent (~ 10 – 20 % of 232-MBO concentrations). Anthropogenic VOC concentrations (which are typically transported into the area from the Colorado Springs or Denver metropolitan areas) are lower than the biogenic signals.

15 A variety of techniques have been used to measure VOCs from different levels on the chemistry tower, individual branches from the dominant vegetation (ponderosa pine), and from the ground. A quadrupole proton transfer reaction mass spectrometer (PTR-MS) measured a suite of selected VOCs (including methanol, acetonitrile, acetaldehyde, acetone + propanal, 232-MBO + isoprene, benzene, monoterpenes and sesquiterpenes) during portions of each of the 2008–2012 growing seasons. Under normal PTR-MS operating conditions, 232-MBO undergoes a dehydration reaction in the PTR-MS drift tube leading to a molecular ion of $m/z = 69$. This is the same ion as protonated isoprene, which is why they are reported as the sum of both species. Measurements alternated between a six point gradient system (1.6, 5, 8.5, 12, 17.7 and 25.1 m above ground) and an eddy covariance (EC) flux system at the top level (25.1 m). In addition, a time-of-flight (TOF) PTR-MS was deployed for EC and concentration measurements above the ponderosa pine canopy in 2010 and 2011 (Kaser et al., 2013a, b). A Selective Reagent Ion (SRI) PTR-TOF-MS instrument was used in

Overview of the Manitou Experimental Forest Observatory

J. Ortega et al.

Title Page

Abstract

Introduction

Conclusions

References

Tables

Figures

⏪

⏩

◀

▶

Back

Close

Full Screen / Esc

Printer-friendly Version

Interactive Discussion



technique at the site (Greenberg et al., 2012). These results suggested that emissions from the litter were negligible, contributing less than 1 % of above-canopy emissions for all BVOCs measured.

A newly developed Thermal desorption Aerosol Gas chromatograph-Aerosol Mass Spectrometer (TAG-AMS) was deployed and analyzed semi-volatile VOCs ($\sim C_{14}-C_{25}$) on a bihourly timescale (Zhao et al., 2013). More than 70 semi-volatile gas-phase species were observed and quantified in the ambient atmosphere during August 2011. Source apportionment was used to identify the origin of these gas-phase species. Some were anthropogenic compounds (such as poly-aromatic hydrocarbons (PAH), oxygenated PAH and alkanes), but 23 species were identified to be terpenoid compounds of biogenic origin from a local source determined from Positive Matrix Factorization (PMF).

In addition to direct VOC emissions and transported species, it is also important to consider oxidation products. These compounds can influence tropospheric ozone formation, oxidative capacity of the atmosphere, and contribute to secondary organic aerosol. Concentrations and fluxes of two important oxygenated VOCs, formaldehyde (HCHO) and glyoxal (CHOCHO), were measured during the 2010 BEACHON-ROCS campaign (DiGangi et al., 2011, 2012) using Fiber Laser-Induced Fluorescence (FILIF; Hottle et al., 2009) and Laser-Induced Phosphorescence (Huisman et al., 2008). Ambient formaldehyde concentrations ranged between a minimum of ~ 0.5 ppb in the early morning hours (4:00 MST), and maximum values of 2–2.5 ppb in the evening ($\sim 20:00$ MST). Ambient glyoxal concentrations ranged between a minimum of ~ 18 ppt in the early morning hours (6:00 MST), and maximum values of 30–55 ppt in the evening ($\sim 17:00$ MST). The glyoxal : formaldehyde ratio maintained a stable diurnal cycle ratio with values of $\sim 1.5-2\%$ in the early morning and at night, and rising to $\sim 2.5-3\%$ in the middle of the days. In addition, to our knowledge, these are the first canopy-scale HCHO eddy flux measurements reported for any site. These results, coupled with enclosure measurements that showed minimal direct emissions, suggest a surprisingly large HCHO production source within the canopy air space. The mid-day HCHO fluxes

Overview of the Manitou Experimental Forest Observatory

J. Ortega et al.

Title Page

Abstract

Introduction

Conclusions

References

Tables

Figures

⏪

⏩

◀

▶

Back

Close

Full Screen / Esc

Printer-friendly Version

Interactive Discussion



were positive (upward) ranging from 37 to 131 $\mu\text{g m}^{-2} \text{h}^{-1}$ (see Fig. 7b) and were correlated with temperature and radiation within the canopy. The missing HCHO source is thus consistent with oxidation of VOCs with light- and temperature-dependent emission profiles. The strength of HCHO fluxes cannot be accounted for by the oxidation of measured MBO and terpenes (also see Sect. 3.2).

3.2 Peroxy and hydroxyl radical observations

Numerous studies (e.g. Stone et al., 2012) have highlighted discrepancies between modeled and measured radical concentrations in forested environments suggesting an incomplete understanding of the chemical processes driving secondary pollutant formation. While most research has focused on regions dominated by isoprene emissions, results from several investigations indicate gaps in our understanding of BVOC oxidation in MBO- and monoterpene-dominated areas similar to MEFO (Kurpius and Goldstein, 2003; Day et al., 2008; Farmer and Cohen, 2008; Wolfe et al., 2011; Mao et al., 2012). Both the 2010 BEACHON-ROCS and 2011 BEACHON-ROMBAS campaigns included measurements of the hydroxyl radical (OH) and peroxy radicals (HO_2 and RO_2) (Table S1), providing a unique opportunity to test our understanding of the chemical reactions that link BVOC oxidation with production of ozone and secondary organic aerosol (SOA) precursors.

Discrepancies between modeled and measured HO_x ($= \text{OH} + \text{HO}_2$) in regions with high BVOC levels have been primarily attributed to “missing” sources of OH (Thornton et al., 2002; Lelieveld et al., 2008; Hofzumahaus et al., 2009; Peeters et al., 2009). In the boundary layer, OH is produced both via “primary” sources, such as photolysis of ozone in the presence of water vapor, and via radical cycling reactions, such as reaction of HO_2 with NO.



Overview of the Manitou Experimental Forest Observatory

J. Ortega et al.

Title Page

Abstract

Introduction

Conclusions

References

Tables

Figures

⏪

⏩

◀

▶

Back

Close

Full Screen / Esc

Printer-friendly Version

Interactive Discussion



Overview of the Manitou Experimental Forest Observatory

J. Ortega et al.

Title Page

Abstract

Introduction

Conclusions

References

Tables

Figures

⏪

⏩

◀

▶

Back

Close

Full Screen / Esc

Printer-friendly Version

Interactive Discussion

In a detailed analysis of OH observations, Kim et al. (2013) demonstrate that radical recycling via reaction (R3) is likely the dominant source of OH within the MEFO canopy. A 0-D box model under-predicts HO_x concentrations relative to observations, implying unidentified sources of HO_2 . Using the same box model in a study focused on peroxy radical observations, Wolfe et al. (2013) confirm this result and identify several potential additional sources of both HO_2 and RO_2 . Notably, it is suggested that oxidation of unmeasured, highly reactive BVOC could explain a significant portion of the missing peroxy radical source. Such a source may also explain the high HCHO fluxes observed during the BEACHON ROCS campaign (DiGangi et al., 2011; see Sect. 3.1). Figure 7a compares the hourly-averaged measured and modeled total peroxy radical mixing ratios for BEACHON-ROCS (August 2010). As described in Wolfe et al. (2013), the difference between measured and modeled values corresponds to a total “missing” peroxy radical production rate of as much as 130 pptmin^{-1} . For comparison, Fig. 7b shows measured and modeled HCHO fluxes (DiGangi et al., 2011). The additional HCHO production needed to reconcile modeled and measured formaldehyde fluxes is on the order of 65 pptmin^{-1} at midday. Uncertainties in measurements and model results contribute to a significant overall uncertainty in these production rate estimates (approximately $\pm 50\%$). Nonetheless, the similarity between these results – obtained via two essentially independent methods – supports the conclusion that VOC oxidation within the canopy is much stronger than predicted by canonical chemical mechanisms.

Analysis of the role of anthropogenic influence on the oxidation of BVOCs, especially via the influence of NO_x on the fate of RO_2 , is of great current interest (Orlando and Tyndall, 2012), and MEFO is well suited for such studies (see also Sect. 4.1). Figure 8a shows the measured HO_2 , $\text{HO}_2 + \text{RO}_2$, NO and NO_2 concentrations during a representative day in BEACHON ROCS (24 August 2010), and Fig. 8c shows the corresponding wind speed and direction. On this day, upslope conditions (that can bring polluted urban air and are often seen at this site; see Fig. 3) were not observed, as the wind was generally out of the south or southwest where there is relatively little anthropogenic influence. During the mid-morning as the boundary layer developed, an

Overview of the Manitou Experimental Forest Observatory

J. Ortega et al.

Title Page

Abstract

Introduction

Conclusions

References

Tables

Figures

⏪

⏩

◀

▶

Back

Close

Full Screen / Esc

Printer-friendly Version

Interactive Discussion



increase in NO_x (Fig. 8a) can be seen, which was likely due to downward transport of a residual layer. The anthropogenic influence on the fate of RO_2 is evident as the loss mechanism was initially dominated by the $\text{RO}_2 + \text{NO}$ channel (Fig. 8b), but during mid-day as NO_x concentrations decreased (due to the residual morning boundary layer breaking up and southwesterly flow to the site), the $\text{RO}_2 + \text{HO}_2$ channel became the major loss mechanism. While the patterns of these transitions do not appreciably affect the concentrations of biogenic and anthropogenic VOCs, the changes in the role of the different reaction channels are consistent with the measured HCHO and glyoxal concentrations (DiGangi et al., 2012) and measured and modeled $\text{HO}_2 + \text{RO}_2$ concentrations indicated in Fig. 7. This competition between NO_x and HO_2 for reaction with the peroxy radicals (RO_2) affects the composition of multigenerational reaction products formed during gas-phase radical cycling and thus dictates, to a large extent, the production of ozone and organic aerosol precursors.

3.3 Aerosol properties and composition

Particle size distribution measurements (covering diameters from 4 nm to 2.5 μm) were conducted for nearly 2 yr at MEFO starting in February 2010 and ending in January 2012. Frequent “small particle events” characterized by high concentrations of 4–20 nm particles were observed, especially during the summer season. The origin of these small particles is likely atmospheric nucleation (Kulmala et al., 2007), which is thought to be caused by reactions of gas-phase sulfuric acid with atmospheric bases such as ammonia and amines as well as oxidized organic compounds (Kirkby et al., 2011; Almeida et al., 2013). An example of three typical small particle events during July 2011 is shown in Fig. 9a, where the onset of each event is seen just prior to noon (MST). These events are common at MEFO in the summer, occurring 3–5 times per week during late morning or early afternoon, and typically coincide with changes in wind speed and direction. Figure 9b shows wind speed and wind direction at the top of the chemistry tower and sulfate aerosol mass loadings measured by the aerosol mass spectrometer. On each of these mornings the wind speed is fairly low ($\sim 1 \text{ ms}^{-1}$) at

75% of the total PM₁ aerosol mass was comprised of organic aerosol (OA), with the rest composed primarily of ammonium sulfate. Nitrate concentrations were low and were shown to be primarily composed of organic nitrates (Fry et al., 2013). Black carbon (BC) aerosol mass was of the order of a few percent of the total submicron mass and more variable, often increasing and decreasing by an order of magnitude on hourly timescales. Transport from urban areas, fires, and local traffic likely explain this high variability. Figure 10b shows the size-resolved composition for the same species and time period. Ammonium and sulfate size distributions were centered at 300–400 nm, while organics and nitrate aerosol size distributions were centered at ~ 250 nm. The distinct size distributions of the chemical components indicate that these aerosols are not completely internally mixed. Figure 10c shows the month-long daily distributions indicating a subtle diurnal cycle in organic aerosol, peaking at night, but with considerable day-to-day variability. The peak in average sulfate (and associated ammonium) at ~ 16:00–19:00 MST is primarily due to the influence of certain days where sulfate increased during late afternoon to early evening with corresponding SO₂ increases (see red spikes in Fig. 10a). The diurnal BC trend has two peaks. The larger of these was in the evening (~ 20:00 MST) coincident with the regular prolonged impact of the urban plume in afternoon through evening and was also seen in other anthropogenic species (e.g. NO_x, CO). The smaller, shorter-duration morning peak (~ 06:00 MST) was also correlated with NO_x and CO. The reason for this morning BC increase could be due to the break-up of the shallow nocturnal boundary layer causing mixing down of more pollution-rich residual layer air, or an increase of local emission sources into a shallow morning boundary layer. It should be noted that the diameter measured from BC aerosol is the mass equivalent diameter (D_{me}) which was obtained by assuming a density of 1.8 g cm⁻³ as recommended by Moteki et al. (2010). The vacuum aerodynamic diameter (D_{va}) shown in the size distributions (Fig. 10b) was computed by multiplying D_{me} by the density (1.8). D_{va} of the particles containing BC could be larger if the BC was internally mixed with other non-BC compounds (e.g. organic coatings), or smaller if the particles had irregular shapes (DeCarlo et al., 2004). BC diameters peaked at D_{va}

Overview of the Manitou Experimental Forest Observatory

J. Ortega et al.

[Title Page](#)[Abstract](#)[Introduction](#)[Conclusions](#)[References](#)[Tables](#)[Figures](#)[Back](#)[Close](#)[Full Screen / Esc](#)[Printer-friendly Version](#)[Interactive Discussion](#)

~ 200–300 nm, which is approximately 100 nm smaller than the peak of the organic and nitrate distributions.

PM_{2.5} collection onto quartz fiber filters during the same campaign were analyzed for a variety of specific SOC (Secondary Organic Carbon) and carbon isotopic measurements as described in Geron (2011) and Lewandowski et al. (2013). These results estimated that 0.5 μgCm⁻³ could be attributed to specific SOC (Secondary Organic Carbon) precursors. Hemiterpene precursor compounds (isoprene + MBO) represented approximately half of the observed SOC, with monoterpenes contributing nearly the same amount to the total SOC. Isotopic measurements of these same filter samples found that the ¹⁴C ratio was 0.71 ± 0.11 (range 0.52 to 0.88), indicating that roughly three quarters of the particulate carbon observed during BEACHON-RoMBAS was of modern, non-petrogenic origin. The fraction of modern carbon (70%) at this site is less than values observed in eastern US forests. For example, Geron (2009) reported mean summer-time values of 83% and with maximum values reaching 97% for those forests. Similarly, during summer months near forests in the Eastern United States, Lewis et al. (2004) observed values between ~ 80–95%. Organic tracer results (including isoprene, MT, and 232-MBO oxidation products) indicate that the lower fraction of contemporary carbon is primarily due to lower total biogenic emissions and lower organic mass loadings and not due to more traffic or other urban influences (Kleindienst et al., 2007). The modern carbon results from MEFO can also be compared to measurements at nine Interagency Monitoring for Protection of Visual Environments (IMPROVE) network sites. The values from the urban sites in this network averaged approximately 50% (Bench et al., 2007).

Gas- and aerosol-phase organic nitrate concentrations were quantified with thermal dissociation, laser-induced fluorescence (TD-LIF; Day et al., 2002; Rollins et al., 2010) during summer 2011 (Fry et al., 2013). Gas-phase organic nitrate classes showed diurnal cycles peaking mid-day at ~ 200 ppt (total alkyl and multifunctional nitrates) ~ 300 ppt (total peroxy acyl nitrates) while total particle-phase organic nitrates peaked at night or early morning. Formation rates of gas-phase organic nitrates within the

Overview of the Manitou Experimental Forest Observatory

J. Ortega et al.

Title Page

Abstract

Introduction

Conclusions

References

Tables

Figures

⏪

⏩

◀

▶

Back

Close

Full Screen / Esc

Printer-friendly Version

Interactive Discussion

Overview of the Manitou Experimental Forest Observatory

J. Ortega et al.

Title Page

Abstract

Introduction

Conclusions

References

Tables

Figures

⏪

⏩

◀

▶

Back

Close

Full Screen / Esc

Printer-friendly Version

Interactive Discussion



shallow nocturnal boundary layer were comparable to daytime formation rates. It was observed that total gas- and particle-phase organic nitrates had equilibrium-like responses to diurnal temperature changes, suggesting some reversible partitioning although thermodynamic modeling could not explain all of the repartitioning. Additionally, diurnal cycles of gas-particle partitioning supported model-predicted nighttime formation of lower volatility products, compared to daytime, from NO_3 radical-initiated oxidation of monoterpenes. Aerosol-phase organic nitrates were also measured by AMS and showed good agreement with TD-LIF (Fry et al., 2013).

Hundreds of acids in the gas and aerosol phases were quantified in real-time during summer 2011 using the newly-developed Micro-Orifice Volatilization Impactor High-Resolution Time-of-Flight Chemical Ionization Mass Spectrometer (MOVI-HRToF-CIMS; Yatavelli et al., 2012, 2013). This technique provides a direct measurement of the gas-particle partitioning of individual and bulk organic acids. Bulk organic acids followed absorptive partitioning, responding to temperature changes on timescales of ~ 1 – 2 h, suggesting there were not major kinetic limitations to species evaporation. Species carbon number and oxygen content, together with ambient temperature, controlled the volatility of organic acids and were good partitioning predictors. Moreover, the relationship between observed and modeled partitioning with carbon number and oxygen content pointed toward the likely importance of different classes of multifunctional organic acids that comprised the bulk of the acid groups (e.g. hydroxyacids, hydroperoxyacids, or polyacids but not ketoacids).

A newly identified 232-MBO-derived organosulfate was identified in aerosol samples during the 2011 BEACHON-RoMBAS study, although at levels significantly lower than reported for a similar ponderosa pine-dominated site in California (Zhang et al., 2012). The reason for the lower organosulfates observed in the aerosol filter samples was tentatively attributed to the lower acidity of the pre-existing aerosol at BEACHON compared to the California site. Acidity is thought to greatly enhance the formation of this organosulfate. This species has the potential to be used as a tracer of SOA formation from 232-MBO.

can influence both CCN and IN. Changes in cloud properties and precipitation can, in turn, influence biogenic emissions, closing the loop on a potentially important feedback between the carbon and water cycles (Pöschl et al., 2010; Morris et al., 2014).

To better understand the influence of biogenic secondary organic aerosol on aerosol hygroscopicity and the seasonal variability of CCN, a continuous 14 month study (March 2010–May 2011) was performed at MEFO (Levin et al., 2012). This was followed by additional measurements during the 2011 BEACHON-RoMBAS intensive campaign, which allowed for direct comparison between aerosol hygroscopicity and aerosol chemical composition measurements (Levin et al., 2013). Aerosol hygroscopicity was described using the dimensionless hygroscopicity parameter, κ (Petters and Kreidenweis, 2007), with an annual averaged κ value of 0.16 ± 0.08 . This value is similar to κ values measured in remote, forested regions, such as in Finland (Cerully et al., 2011) and the Brazilian Amazon (Gunthe et al., 2009), and is lower than the commonly assumed continental value of $\kappa = 0.3$ (Andreae and Rosenfeld, 2008). Aerosol composition derived from the hygroscopicity measurements at MEFO indicated a predominance of organic species in the aerosol, leading to the low κ measurement values. Direct comparison of organic mass fraction measured by aerosol mass spectrometry and filter measurements (discussed in Sect. 3.3) during BEACHON-RoMBAS agreed well with the composition derived from the hygroscopicity measurements. Organic mass fractions were found to be largest (up to 90 %) in the smallest particles (20–30 nm) as measured by a Thermal Desorption Chemical Ionization Mass Spectrometer (TDCIMS). This fraction decreased with increasing particle diameter as measured by the AMS (Fig. 10b; Levin et al., 2013), and is consistent with the smallest particles being composed primarily of oxidized organic species from forest emissions. Results from the year-long measurements showed that κ was slightly higher during the winter months when biogenic emissions (which are strongly temperature-dependent) are suppressed. The combination of these results suggests that secondary organic aerosol derived from biogenic emissions impact aerosol hygroscopicity and CCN number concentrations throughout the year.

Overview of the Manitou Experimental Forest Observatory

J. Ortega et al.

[Title Page](#)[Abstract](#)[Introduction](#)[Conclusions](#)[References](#)[Tables](#)[Figures](#)[⏪](#)[⏩](#)[◀](#)[▶](#)[Back](#)[Close](#)[Full Screen / Esc](#)[Printer-friendly Version](#)[Interactive Discussion](#)

Overview of the Manitou Experimental Forest Observatory

J. Ortega et al.

Title Page

Abstract

Introduction

Conclusions

References

Tables

Figures

⏪

⏩

◀

▶

Back

Close

Full Screen / Esc

Printer-friendly Version

Interactive Discussion

can be addressed. For example, how are the oxidation pathways of locally emitted BVOC influenced by oxidant levels (NO_3 , OH and O_3) during clean and polluted conditions? In addition, to what extent does the transport of SO_2 , oxidants and VOCs from urban areas affect particle nucleation and growth? Model simulations can be initialized and parameterized using long-term and campaign-specific measurements of aerosols, VOCs, trace gasses, and meteorology. Results from these simulations can then be compared to observations. Local emissions are dominated by 232-MBO and monoterpenes, but these can be augmented by transport of anthropogenic species from the Front Range cities. Typical summertime ozone concentrations are 50–60 ppb during the afternoon, and decrease to ~ 10 –20 ppb at night. Nitrogen oxides (NO_x) are generally dominated by NO_2 with typical values ~ 0.5 to 4 ppb, although occasional urban influences can cause the concentration to increase to 8–10 ppb. NO concentrations are much lower – typically less than 500 ppt, and rarely exceed 1 ppb. Since the area is relatively rural with low NO_x concentrations, ozone is not titrated away at night as would typically happen in an urban environment. Average SO_2 concentrations are quite low year-round, averaging less than 200 ppt, but concentrations can occasionally spike to ~ 2 ppb. The average July 2011 CO concentration was 100 ppb (standard deviation of 5.2 ppb). These values increase when urban air is transported to the site, but rarely exceed 150 ppb. CO measurements taken at other times of year have shown similar consistent results. Figures 3 and 6 above demonstrate the concentrations of some of these gas-phase species. These direct measurements provide valuable insight into the range of atmospheric conditions that the site experiences, and can be used as initial inputs and provide constraints in modeling efforts. The relatively clean conditions combined with periodic, well-defined urban perturbations make it an ideally situated location for studying atmospheric processes at the rural-urban interface. An example of this was demonstrated in Fig. 8 (adapted from DiGangi et al., 2012), which shows the ambient concentrations of HO_2 , RO_2 , NO and NO_2 in 8A and the corresponding wind speed and direction in 8C during a representative BEACHON-ROCS day (24 August 2010). In the early morning, both HO_2 and RO_2 are very low (< 20 ppt), accompanied by low wind

Overview of the Manitou Experimental Forest Observatory

J. Ortega et al.

Title Page

Abstract

Introduction

Conclusions

References

Tables

Figures

⏪

⏩

◀

▶

Back

Close

Full Screen / Esc

Printer-friendly Version

Interactive Discussion

mation of secondary organic aerosols by nighttime NO_3 chemistry, increased OH and O_3 oxidation, or the direct transport of anthropogenic OA to the site. NO_3 chemistry contributes to larger SOA concentrations at night when the boundary layer is shallow (Fry et al., 2013), but the overall contribution to the actual aerosol column relevant to radiative forcing is small (a $1 \mu\text{g m}^{-3}$ mass concentration represents a $100 \mu\text{g m}^{-2}$ column density in a 100 m nighttime boundary layer). Daytime aerosol mass loadings contribute much more to the regional aerosol mass due to the combination of the higher mass loadings and fully developed boundary layer ($2 \mu\text{g m}^{-3}$ corresponds to $4000 \mu\text{g m}^{-2}$ in a 2 km daytime boundary layer; a forty-fold increase column height).

Small particle events were often correlated with elevated SO_2 concentrations. Figure 13 shows the onset and subsequent growth of particles at the site during one of these events (29 July 2011) as observed (a) and the corresponding WRF-Chem simulation (b). Model results indicate that initial particle formation is triggered by anthropogenic SO_2 , whereas subsequent particle growth is driven by condensation of BVOC oxidation products as discussed in Sect. 3.3. Growth rates were calculated using the number mean diameter defined by (Matsui et al., 2011):

$$\text{NMD} = \frac{\sum_i D p_i \times N_i}{\sum_i N_i} \quad (1)$$

where $D p_i$ and N_i are the diameter (nm) and number concentration respectively. The model simulations estimated that the average particle growth rates during these events (from 4–40 nm mobility diameter) were 3.4 nm h^{-1} . The observed values calculated from SMPS measurements (average = 2.0 nm h^{-1}) are less than the simulated values, but in reasonable agreement with other reports from forested regions in Indiana USA (2.5 nm h^{-1} ; Pryor et al., 2010) and Finland (2.9 nm h^{-1} ; Jaatinen et al., 2009). It should also be noted that there is considerable variability in reported growth rates, and this value is highly dependent upon the chosen diameter range.

The impact of biogenic aerosols on clouds and precipitation was also investigated as part of the BEACHON project. Figure 13c shows the effect of new particle formation

model parameterization and evaluation studies. The infrastructure exists to enable additional measurements and future scientific measurement campaigns as well as for testing new instruments, measurement inter-comparisons, graduate and undergraduate student development and other studies involving terrestrial-atmospheric exchange processes. MEFO is a collaborative facility that is maintained through a cooperative agreement between NCAR and the USDA Forest Service and is available to the scientific community for training, model development and evaluation and scientific discovery.

Supplementary material related to this article is available online at <http://www.atmos-chem-phys-discuss.net/14/1647/2014/acpd-14-1647-2014-supplement.pdf>.

Acknowledgements. The authors would like to acknowledge generous field support from Richard Oakes (USDA Forest Service, Manitou Experimental Forest Site Manager). Authors from Colorado State University were supported through NSF grant ATM-0919042. Authors from the University of Colorado were supported by NSF grant ATM-0919189 and United States Department of Energy grant DE-SC0006035. Authors from the National Center for Atmospheric Research were supported by NSF grant ATM-0919317 and US Department of Energy grant DE-SC00006861. Thomas Karl was also supported by the EC Seventh Framework Program (Marie Curie Reintegration Program, "ALP-AIR", grant no. 334084). S. C. Pryor (Indiana University) was supported by NSF ATM-1102309. Authors from the University of Innsbruck were supported by the Austrian Science Fund (FWF) under the project number L518-N20.L. Kaser was also supported from a DOC-fFORTE-fellowship of the Austrian Academy of Science. Authors from the University of Wisconsin-Madison were supported by NSF grant ATM-0852406, the BEACHON project and NASA-SBIR Phase I & II funding. Contributions from Los Alamos National Laboratory (LANL) were funded by the United States Department of Energy's Atmospheric System Research (Project F265, KP1701, M. K. Dubey principal investigator). A. C. Aiken also thanks LANL – Laboratory Directed Research and Development for a Director's postdoctoral fellowship award. The authors would also like to acknowledge substantial participation and input from the Max Planck Institute for Chemistry (MPIC; Mainz, Germany), which was funded by the Max Planck Society (MPG) and the Geocycles Cluster Mainz (LEC Rheinland-Pfalz).

**Overview of the
Manitou
Experimental Forest
Observatory**

J. Ortega et al.

Title Page

Abstract

Introduction

Conclusions

References

Tables

Figures



Back

Close

Full Screen / Esc

Printer-friendly Version

Interactive Discussion



Overview of the Manitou Experimental Forest Observatory

J. Ortega et al.

Title Page

Abstract

Introduction

Conclusions

References

Tables

Figures

◀

▶

◀

▶

Back

Close

Full Screen / Esc

Printer-friendly Version

Interactive Discussion

Alo, C. A. and Wang, G. L.: Hydrological impact of the potential future vegetation response to climate changes projected by 8 GCMs, *J. Geophys. Res.-Biogeo.*, 113, 16, doi:10.1029/2007jg000598, 2008.

Andreae, M. O. and Rosenfeld, D.: Aerosol-cloud-precipitation interactions, Part 1 the nature and sources of cloud-active aerosols, *Earth Sci. Rev.*, 89, 13–41, doi:10.1016/j.earscirev.2008.03.001, 2008.

Apel, E. C., Emmons, L. K., Karl, T., Flocke, F., Hills, A. J., Madronich, S., Lee-Taylor, J., Fried, A., Weibring, P., Walega, J., Richter, D., Tie, X., Mauldin, L., Campos, T., Weinheimer, A., Knapp, D., Sive, B., Kleinman, L., Springston, S., Zaveri, R., Ortega, J., Voss, P., Blake, D., Baker, A., Warneke, C., Welsh-Bon, D., de Gouw, J., Zheng, J., Zhang, R., Rudolph, J., Junkermann, W., and Riemer, D. D.: Chemical evolution of volatile organic compounds in the outflow of the Mexico City Metropolitan area, *Atmos. Chem. Phys.*, 10, 2353–2375, doi:10.5194/acp-10-2353-2010, 2010.

Barth, M., McFadden, J. P., Sun, J. L., Wiedinmyer, C., Chuang, P., Collins, D., Griffin, R., Hannigan, M., Karl, T., Kim, S. W., Lasher-Trapp, S., Levis, S., Litvak, M., Mahowald, N., Moore, K., Nandi, S., Nemitz, E., Nenes, A., Potosnak, M., Raymond, T. M., Smith, J., Still, C., and Stroud, C.: Coupling between land ecosystems and the atmospheric hydrologic cycle through biogenic aerosol pathways, *B. Am. Meteorol. Soc.*, 86, 1738–1742, doi:10.1175/bams-86-12-1738, 2005.

Battaglia, M. A., Rocca, M. E., Rhoades, C. C., and Ryan, M. G.: Surface fuel loadings within mulching treatments in Colorado coniferous forests, *Forest Ecol. Manag.*, 260, 1557–1566, doi:10.1016/j.foreco.2010.08.004, 2010.

Beier, C., Beierkuhnlein, C., Wohlgemuth, T., Penuelas, J., Emmett, B., Korner, C., de Boeck, H. J., Christensen, J. H., Leuzinger, S., Janssens, I. A., and Hansen, K.: Precipitation manipulation experiments – challenges and recommendations for the future, *Ecol. Lett.*, 15, 899–911, doi:10.1111/j.1461-0248.2012.01793.x, 2012.

Bench, G., Fallon, S., Schichtel, B., Malm, W., and McDade, C.: Relative contributions of fossil and contemporary carbon sources to PM_{2.5} aerosols at nine Interagency Monitoring for Protection of Visual Environments (IMPROVE) network sites, *J. Geophys. Res.-Atmos.*, 112, 10, doi:10.1029/2006jd007708, 2007.

Berkelhammer, M., Hu, J., Bailey, A., Noone, D. C., Still, C., Barnard, H., Gochis, D., Hsiao, G. S., Rahn, T., and Turnipseed, A.: The nocturnal water cycle in an open-canopy forest. *J. Geophys. Res.-Atmos.*, 118, 10225–10242, doi:10.1002/jgrd.50701, 2013.

Overview of the Manitou Experimental Forest Observatory

J. Ortega et al.

Title Page

Abstract

Introduction

Conclusions

References

Tables

Figures

◀

▶

◀

▶

Back

Close

Full Screen / Esc

Printer-friendly Version

Interactive Discussion

- Burgess, S. S. O., Adams, M. A., Turner, N. C., Beverly, C. R., Ong, C. K., Khan, A. A. H., and Bleby, T. M.: An improved heat pulse method to measure low and reverse rates of sap flow in woody plants, *Tree Physiol.*, 21, 589–598, 2001.
- Carlsaw, K. S., Boucher, O., Spracklen, D. V., Mann, G. W., Rae, J. G. L., Woodward, S., and Kulmala, M.: A review of natural aerosol interactions and feedbacks within the Earth system, *Atmos. Chem. Phys.*, 10, 1701–1737, doi:10.5194/acp-10-1701-2010, 2010.
- Cerully, K. M., Raatikainen, T., Lance, S., Tkacik, D., Tiitta, P., Petäjä, T., Ehn, M., Kulmala, M., Worsnop, D. R., Laaksonen, A., Smith, J. N., and Nenes, A.: Aerosol hygroscopicity and CCN activation kinetics in a boreal forest environment during the 2007 EUCAARI campaign, *Atmos. Chem. Phys.*, 11, 12369–12386, doi:10.5194/acp-11-12369-2011, 2011.
- Constantinidou, H. A., Hirano, S. S., Baker, L. S., Upper, C. D.: Atmospheric dispersal of ice nucleation-active bacteria: the role of rain, *Phytopathology*, 80, 934–937, 1990.
- Cross, E. S., Hunter, J. F., Carrasquillo, A. J., Franklin, J. P., Herndon, S. C., Jayne, J. T., Worsnop, D. R., Miake-Lye, R. C., and Kroll, J. H.: Online measurements of the emissions of intermediate-volatility and semi-volatile organic compounds from aircraft, *Atmos. Chem. Phys.*, 13, 7845–7858, doi:10.5194/acp-13-7845-2013, 2013.
- Day, D. A., Wooldridge, P. J., Dillon, M. B., Thornton, J. A., and Cohen, R. C.: A thermal dissociation laser-induced fluorescence instrument for in situ detection of NO₂, peroxy nitrates, alkyl nitrates, and HNO₃, *J. Geophys. Res.-Atmos.*, 107, 14, doi:10.1029/2001jd000779, 2002.
- Day, D. A., Wooldridge, P. J., and Cohen, R. C.: Observations of the effects of temperature on atmospheric HNO₃, Σ ANs, Σ PNs, and NO_x: evidence for a temperature-dependent HO_x source, *Atmos. Chem. Phys.*, 8, 1867–1879, doi:10.5194/acp-8-1867-2008, 2008.
- DeCarlo, P. F., Kimmel, J. R., Trimborn, A., Northway, M. J., Jayne, J. T., Aiken, A. C., Gonin, M., Fuhrer, K., Horvath, T., Docherty, K. S., Worsnop, D. R., and Jimenez, J. L.: Field-deployable, high-resolution, time-of-flight aerosol mass spectrometer, *Anal. Chem.*, 78, 8281–8289, doi:10.1021/ac061249n, 2006.
- DeMott, P. J. and Prenni, A. J.: New directions: need for defining the numbers and sources of biological aerosols acting as ice nuclei, *Atmos. Environ.*, 44, 1944–1945, doi:10.1016/j.atmosenv.2010.02.032, 2010a.
- DeMott, P. J., Prenni, A. J., Liu, X., Kreidenweis, S. M., Petters, M. D., Twohy, C. H., Richardson, M. S., Eidhammer, T., and Rogers, D. C.: Predicting global atmospheric ice nuclei distributions and their impacts on climate, *P. Natl. Acad. Sci. USA*, 107, 11217–11222, doi:10.1073/pnas.0910818107, 2010b.

Overview of the Manitou Experimental Forest Observatory

J. Ortega et al.

Title Page

Abstract

Introduction

Conclusions

References

Tables

Figures

◀

▶

◀

▶

Back

Close

Full Screen / Esc

Printer-friendly Version

Interactive Discussion

Denman, K. L., Brasseur, G., Chidthaisong, A., Ciais, P., Cox, P. M., Dickinson, R. E., Hauglustaine, D., Heinze, C., Holland, E., Jacob, D., Lohmann, U., Ramachandran, S., da Silva Dias, P. L., Wofsy, S. C., and Zhang, X.: Couplings Between Changes in the Climate System and Biogeochemistry, in: *Climate Change 2007: The Physical Science Basis. Contribution of Working Group I to the Fourth Assessment Report of the Intergovernmental Panel on Climate Change*, edited by: Solomon, S., Qin, D., Manning, M., Chen, Z., Marquis, M., Averyt, K. B., Tignor, M., and Miller, H. L., Cambridge University Press, Cambridge, United Kingdom and New York, NY, USA, 2007.

DiGangi, J. P., Boyle, E. S., Karl, T., Harley, P., Turnipseed, A., Kim, S., Cantrell, C., Maudlin III, R. L., Zheng, W., Flocke, F., Hall, S. R., Ullmann, K., Nakashima, Y., Paul, J. B., Wolfe, G. M., Desai, A. R., Kajii, Y., Guenther, A., and Keutsch, F. N.: First direct measurements of formaldehyde flux via eddy covariance: implications for missing in-canopy formaldehyde sources, *Atmos. Chem. Phys.*, 11, 10565–10578, doi:10.5194/acp-11-10565-2011, 2011.

DiGangi, J. P., Henry, S. B., Kammrath, A., Boyle, E. S., Kaser, L., Schnitzhofer, R., Graus, M., Turnipseed, A., Park, J.-H., Weber, R. J., Hornbrook, R. S., Cantrell, C. A., Maudlin III, R. L., Kim, S., Nakashima, Y., Wolfe, G. M., Kajii, Y., Apel, E.C., Goldstein, A. H., Guenther, A., Karl, T., Hansel, A., and Keutsch, F. N.: Observations of glyoxal and formaldehyde as metrics for the anthropogenic impact on rural photochemistry, *Atmos. Chem. Phys.*, 12, 9529–9543, doi:10.5194/acp-12-9529-2012, 2012.

Dube, W. P., Brown, S. S., Osthoff, H. D., Nunley, M. R., Ciciora, S. J., Paris, M. W., McLaughlin, R. J., and Ravishankara, A. R.: Aircraft instrument for simultaneous, in situ measurement of NO_3 and N_2O_5 via pulsed cavity ring-down spectroscopy, *Rev. Sci. Instrum.*, 77, 11, doi:10.1063/1.2176058, 2006.

Eisele, F. L. and Tanner, D. J.: Ion-assisted tropospheric OH measurements, *J. Geophys. Res.-Atmos.*, 96, 9295–9308, doi:10.1029/91jd00198, 1991.

Eisele, F. L. and Tanner, D. J.: Measurement of the gas-phase concentration of H_2SO_4 and methane sulfonic acid and estimates of H_2SO_4 production and loss in the atmosphere, *J. Geophys. Res.-Atmos.*, 98, 9001–9010, doi:10.1029/93jd00031, 1993.

Elbert, W., Taylor, P. E., Andreae, M. O., and Pöschl, U.: Contribution of fungi to primary biogenic aerosols in the atmosphere: wet and dry discharged spores, carbohydrates, and inorganic ions, *Atmos. Chem. Phys.*, 7, 4569–4588, doi:10.5194/acp-7-4569-2007, 2007.

Overview of the Manitou Experimental Forest Observatory

J. Ortega et al.

Title Page

Abstract

Introduction

Conclusions

References

Tables

Figures

◀

▶

◀

▶

Back

Close

Full Screen / Esc

Printer-friendly Version

Interactive Discussion

- Eller, A. S. D., Harley, P., and Monson, R. K.: Potential contribution of exposed resin to ecosystem emissions of monoterpenes, *Atmos. Environ.*, 77, 440–444, 2013.
- Farmer, D. K. and Cohen, R. C.: Observations of HNO_3 , ΣAN , ΣPN and NO_2 fluxes: evidence for rapid HO_x chemistry within a pine forest canopy, *Atmos. Chem. Phys.*, 8, 3899–3917, doi:10.5194/acp-8-3899-2008, 2008.
- Fast, J. D., Gustafson, W. I., Easter, R. C., Zaveri, R. A., Barnard, J. C., Chapman, E. G., Grell, G. A., and Peckham, S. E.: Evolution of ozone, particulates, and aerosol direct radiative forcing in the vicinity of Houston using a fully coupled meteorology-chemistry-aerosol model, *J. Geophys. Res.-Atmos.*, 111, D21305, doi:10.1029/2005jd006721, 2006.
- Fornwalt, P. J., Kaufmann, M. R., and Stohlgren, T. J.: Impacts of mixed severity wildfire on exotic plants in a Colorado ponderosa pine-Douglas-fir forest, *Biol. Invasions*, 12, 2683–2695, doi:10.1007/s10530-009-9674-2, 2010.
- Fry, J. L., Draper, D. C., Zarzana, K. J., Campuzano-Jost, P., Day, D. A., Jimenez, J. L., Brown, S. S., Cohen, R. C., Kaser, L., Hansel, A., Cappellin, L., Karl, T., Hodzic Roux, A., Turnipseed, A., Cantrell, C., Lefer, B. L., and Grossberg, N.: Observations of gas- and aerosol-phase organic nitrates at BEACHON-RoMBAS 2011, *Atmos. Chem. Phys.*, 13, 8585–8605, doi:10.5194/acp-13-8585-2013, 2013.
- Gary, H. L.: A Summary of Research at the Manitou Experimental Forest in Colorado, 1937–1983, US Department of Agriculture, Forest Service Publication, Rocky Mountain Forest and Range Experiment Station, Fort Collins, CO, 1985.
- Geron, C.: Carbonaceous aerosol over a Pinus taeda forest in Central North Carolina, USA, *Atmos. Environ.*, 43, 959–969, doi:10.1016/j.atmosenv.2008.10.053, 2009.
- Geron, C.: Carbonaceous aerosol characteristics over a Pinus taeda plantation: results from the CELTIC experiment, *Atmos. Environ.*, 45, 794–801, doi:10.1016/j.atmosenv.2010.07.015, 2011.
- Greenberg, J. P., Asensio, D., Turnipseed, A., Guenther, A. B., Karl, T., and Gochis, D.: Contribution of leaf and needle litter to whole ecosystem BVOC fluxes, *Atmos. Environ.*, 59, 302–311, doi:10.1016/j.atmosenv.2012.04.038, 2012.
- Grell, G. A., Peckham, S. E., Schmitz, R., McKeen, S. A., Frost, G., Skamarock, W. C., and Elder, B.: Fully coupled “online” chemistry within the WRF model, *Atmos. Environ.*, 39, 6957–6975, doi:10.1016/j.atmosenv.2005.04.027, 2005.
- Gunthe, S. S., King, S. M., Rose, D., Chen, Q., Roldin, P., Farmer, D. K., Jimenez, J. L., Artaxo, P., Andreae, M. O., Martin, S. T., and Pöschl, U.: Cloud condensation nuclei in

Overview of the Manitou Experimental Forest Observatory

J. Ortega et al.

Title Page

Abstract

Introduction

Conclusions

References

Tables

Figures

◀

▶

◀

▶

Back

Close

Full Screen / Esc

Printer-friendly Version

Interactive Discussion

pristine tropical rainforest air of Amazonia: size-resolved measurements and modeling of atmospheric aerosol composition and CCN activity, *Atmos. Chem. Phys.*, 9, 7551–7575, doi:10.5194/acp-9-7551-2009, 2009.

5 Guenther, A., Kulmala, M., Turnipseed, A., Rinne, J., Suni, T., and Reissell, A.: Integrated land ecosystem-atmosphere processes study (iLEAPS) assessment of global observational networks, *Boreal Environ. Res.*, 16, 321–336, 2011.

Haman, C. L., Lefer, B., and Morris, G. A.: Seasonal variability in the diurnal evolution of the boundary layer in a near-coastal urban environment, *J. Atmos. Ocean. Tech.*, 29, 697–710, doi:10.1175/jtech-d-11-00114.1, 2012.

10 Harley, P., Fridd-Stroud, V., Greenberg, J., Guenther, A., and Vasconcellos, P.: Emission of 2-methyl-3-buten-2-ol by pines: a potentially large natural source of reactive carbon to the atmosphere, *J. Geophys. Res.-Atmos.*, 103, 25479–25486, doi:10.1029/98jd00820, 1998.

Heald, C. L., Wilkinson, M. J., Monson, R. K., Alo, C. A., Wang, G. L., and Guenther, A.: Response of isoprene emission to ambient CO₂ changes and implications for global budgets, *Glob. Change Biol.*, 15, 1127–1140, doi:10.1111/j.1365-2486.2008.01802.x, 2009.

15 Hoffmann, T., Bandur, R., Hoffmann, S., and Warscheid, B.: On-line characterization of gaseous and particulate organic analytes using atmospheric pressure chemical ionization mass spectrometry, *Spectrochim. Acta B*, 57, 1635–1647, doi:10.1016/s0584-8547(02)00111-8, 2002.

20 Hofzumahaus, A., Rohrer, F., Lu, K. D., Bohn, B., Brauers, T., Chang, C. C., Fuchs, H., Holland, F., Kita, K., Kondo, Y., Li, X., Lou, S. R., Shao, M., Zeng, L. M., Wahner, A., and Zhang, Y. H.: Amplified trace gas removal in the Troposphere, *Science*, 324, 1702–1704, doi:10.1126/science.1164566, 2009.

Hottle, J. R., Huisman, A. J., Digangi, J. P., Kammrath, A., Galloway, M. M., Coens, K. L., Keutsch, F. N.: A laser induced fluorescence-based instrument for in-situ measurements of atmospheric formaldehyde, *Environ. Sci. Technol.*, 43, 790–795, doi:10.1021/es801621f, 2009.

25 Huffman, J. A., Docherty, K. S., Aiken, A. C., Cubison, M. J., Ulbrich, I. M., DeCarlo, P. F., Sueper, D., Jayne, J. T., Worsnop, D. R., Ziemann, P. J., and Jimenez, J. L.: Chemically-resolved aerosol volatility measurements from two megacity field studies, *Atmos. Chem. Phys.*, 9, 7161–7182, doi:10.5194/acp-9-7161-2009, 2009.

30 Huffman, J. A., Prenni, A. J., DeMott, P. J., Pöhlker, C., Mason, R. H., Robinson, N. H., Fröhlich-Nowoisky, J., Tobo, Y., Després, V. R., Garcia, E., Gochis, D. J., Harris, E., Müller-Germann, I., Ruzene, C., Schmer, B., Sinha, B., Day, D. A., Andreae, M. O., Jimenez, J. L.,

Overview of the Manitou Experimental Forest Observatory

J. Ortega et al.

[Title Page](#)[Abstract](#)[Introduction](#)[Conclusions](#)[References](#)[Tables](#)[Figures](#)[⏪](#)[⏩](#)[◀](#)[▶](#)[Back](#)[Close](#)[Full Screen / Esc](#)[Printer-friendly Version](#)[Interactive Discussion](#)

Gallagher, M., Kreidenweis, S. M., Bertram, A. K., and Pöschl, U.: High concentrations of biological aerosol particles and ice nuclei during and after rain, *Atmos. Chem. Phys.*, 13, 6151–6164, doi:10.5194/acp-13-6151-2013, 2013.

Huisman, A. J., Hottle, J. R., Coens, K. L., DiGangi, J. P., Galloway, M. M., Kammrath, A., and Keutsch, F. N.: Laser-induced phosphorescence for the in situ detection of glyoxal at part per trillion mixing ratios, *Anal. Chem.*, 80, 5884–5891, doi:10.1021/ac800407b, 2008.

Jaatinen, A., Hamed, A., Joutsensaari, J., Mikkonen, S., Birmili, W., Wehner, B., Spindler, G., Wiedensohler, A., Decesari, S., Mircea, M., Facchini, M. C., Junninen, H., Kulmala, M., Lehtinen, K. E. J., and Laaksonen, A.: A comparison of new particle formation events in the boundary layer at three different sites in Europe, *Boreal Environ. Res.*, 14, 481–498, 2009.

Jones, A. M. and Harrison, R. M.: The effects of meteorological factors on atmospheric bioaerosol concentrations – a review, *Sci. Total Environ.*, 326, 151–180, doi:10.1016/j.scitotenv.2003.11.021, 2004.

Kang, E., Root, M. J., Toohey, D. W., and Brune, W. H.: Introducing the concept of Potential Aerosol Mass (PAM), *Atmos. Chem. Phys.*, 7, 5727–5744, doi:10.5194/acp-7-5727-2007, 2007.

Karl, T., Potosnak, M., Guenther, A., Clark, D., Walker, J., Herrick, J. D., and Geron, C.: Exchange processes of volatile organic compounds above a tropical rain forest: implications for modeling tropospheric chemistry above dense vegetation, *J. Geophys. Res.-Atmos.*, 109, D18306, doi:10.1029/2004jd004738, 2004.

Karl, T., Hansel, A., Cappellin, L., Kaser, L., Herdinger-Blatt, I., and Jud, W.: Selective measurements of isoprene and 2-methyl-3-buten-2-ol based on NO_+ ionization mass spectrometry, *Atmos. Chem. Phys.*, 12, 11877–11884, doi:10.5194/acp-12-11877-2012, 2012.

Karl, T., Kaser, L., and Turnipseed, A.: Eddy covariance measurements of isoprene and 232-MBO based on NO_+ time-of-flight mass spectrometry, *Int. J. Mass Spectrom.*, in press, 2014.

Kaser, L., Karl, T., Schnitzhofer, R., Graus, M., Herdinger-Blatt, I. S., DiGangi, J. P., Sive, B., Turnipseed, A., Hornbrook, R. S., Zheng, W., Flocke, F. M., Guenther, A., Keutsch, F. N., Apel, E., and Hansel, A.: Comparison of different real time VOC measurement techniques in a ponderosa pine forest, *Atmos. Chem. Phys.*, 13, 2893–2906, doi:10.5194/acp-13-2893-2013, 2013a.

Kaser, L., Karl, T., Guenther, A., Graus, M., Schnitzhofer, R., Turnipseed, A., Fischer, L., Harley, P., Madronich, M., Gochis, D., Keutsch, F. N., and Hansel, A.: Undisturbed and disturbed above canopy ponderosa pine emissions: PTR-TOF-MS measurements and MEGAN

**Overview of the
Manitou
Experimental Forest
Observatory**

J. Ortega et al.

Title Page

Abstract

Introduction

Conclusions

References

Tables

Figures

◀

▶

◀

▶

Back

Close

Full Screen / Esc

Printer-friendly Version

Interactive Discussion

2.1 model results, *Atmos. Chem. Phys.*, 13, 11935–11947, doi:10.5194/acp-13-11935-2013, 2013b.

Kleindienst, T. E., Jaoui, M., Lewandowski, M., Offenberg, J. H., Lewis, C. W., Bhave, P. V., and Edney, E. O.: Estimates of the contributions of biogenic and anthropogenic hydrocarbons to secondary organic aerosol at a southeastern US location, *Atmos. Environ.*, 41, 8288–8300, doi:10.1016/j.atmosenv.2007.06.045, 2007.

Kim, S., Karl, T., Guenther, A., Tyndall, G., Orlando, J., Harley, P., Rasmussen, R., and Apel, E.: Emissions and ambient distributions of Biogenic Volatile Organic Compounds (BVOC) in a ponderosa pine ecosystem: interpretation of PTR-MS mass spectra, *Atmos. Chem. Phys.*, 10, 1759–1771, doi:10.5194/acp-10-1759-2010, 2010.

Kim, S., Wolfe, G. M., Mauldin, L., Cantrell, C., Guenther, A., Karl, T., Turnipseed, A., Greenberg, J., Hall, S. R., Ullmann, K., Apel, E., Hornbrook, R., Kajii, Y., Nakashima, Y., Keutsch, F. N., DiGangi, J. P., Henry, S. B., Kaser, L., Schnitzhofer, R., Graus, M., Hansel, A., Zheng, W., and Flocke, F. F.: Evaluation of HO_x sources and cycling using measurement-constrained model calculations in a 2-methyl-3-butene-2-ol (MBO) and monoterpene (MT) dominated ecosystem, *Atmos. Chem. Phys.*, 13, 2031–2044, doi:10.5194/acp-13-2031-2013, 2013.

Kirkby, J., Curtius, J., Almeida, J., Dunne, E., Duplissy, J., Ehrhart, S., Franchin, A., Gagne, S., Ickes, L., Kurten, A., Kupc, A., Metzger, A., Riccobono, F., Rondo, L., Schobesberger, S., Tsagkogeorgas, G., Wimmer, D., Amorim, A., Bianchi, F., Breitenlechner, M., David, A., Dommen, J., Downard, A., Ehn, M., Flagan, R. C., Haider, S., Hansel, A., Hauser, D., Jud, W., Junninen, H., Kreissl, F., Kvashin, A., Laaksonen, A., Lehtipalo, K., Lima, J., Lovejoy, E. R., Makhmutov, V., Mathot, S., Mikkila, J., Minginette, P., Mogo, S., Nieminen, T., Onnela, A., Pereira, P., Petaja, T., Schnitzhofer, R., Seinfeld, J. H., Sipila, M., Stozhkov, Y., Stratmann, F., Tome, A., Vanhanen, J., Viisanen, Y., Vrtala, A., Wagner, P. E., Walther, H., Weingartner, E., Wex, H., Winkler, P. M., Carslaw, K. S., Worsnop, D. R., Baltensperger, U., and Kulmala, M.: Role of sulphuric acid, ammonia and galactic cosmic rays in atmospheric aerosol nucleation, *Nature*, 476, 429–U477, doi:10.1038/nature10343, 2011.

Kleindienst, T. E., Jaoui, M., Lewandowski, M., Offenberg, J. H., Lewis, C. W., Bhave, P. V., and Edney, E. O.: Estimates of the contributions of biogenic and anthropogenic hydrocarbons to secondary organic aerosol at a southeastern US location, *Atmos. Environ.*, 41, 8288–8300, doi:10.1016/j.atmosenv.2007.06.045, 2007.

Overview of the Manitou Experimental Forest Observatory

J. Ortega et al.

Title Page

Abstract

Introduction

Conclusions

References

Tables

Figures

⏪

⏩

◀

▶

Back

Close

Full Screen / Esc

Printer-friendly Version

Interactive Discussion

- Kulmala, M., Riipinen, I., Sipila, M., Manninen, H. E., Petaja, T., Junninen, H., Dal Maso, M., Mordas, G., Mirme, A., Vana, M., Hirsikko, A., Laakso, L., Harrison, R. M., Hanson, I., Leung, C., Lehtinen, K. E. J., and Kerminen, V. M.: Toward direct measurement of atmospheric nucleation, *Science*, 318, 89–92, doi:10.1126/science.1144124, 2007.
- 5 Kurpius, M. R. and Goldstein, A. H.: Gas-phase chemistry dominates O₃ loss to a forest, implying a source of aerosols and hydroxyl radicals to the atmosphere, *Geophys. Res. Lett.*, 30, 1371, doi:10.1029/2002gl016785, 2003.
- Lelieveld, J., Butler, T. M., Crowley, J. N., Dillon, T. J., Fischer, H., Ganzeveld, L., Harder, H., Lawrence, M. G., Martinez, M., Taraborrelli, D., and Williams, J.: Atmospheric oxidation capacity sustained by a tropical forest, *Nature*, 452, 737–740, doi:10.1038/nature06870, 2008.
- 10 Levin, E. J. T., Prenni, A. J., Petters, M. D., Kreidenweis, S. M., Sullivan, R. C., Atwood, S. A., Ortega, J., DeMott, P. J., and Smith, J. N.: An annual cycle of size-resolved aerosol hygroscopicity at a forested site in Colorado, *J. Geophys. Res.-Atmos.*, 117, D06201, doi:10.1029/2011jd016854, 2012.
- 15 Levin, E. J. T., Prenni, A. J., Palm, B., Day, D., Campuzano-Jost, P., Winkler, P. M., Kreidenweis, S. M., DeMott, P. J., Jimenez, J., and Smith, J. N.: Size-resolved aerosol composition and link to hygroscopicity at a forested site in Colorado, *Atmos. Chem. Phys. Discuss.*, 13, 23817–23843, doi:10.5194/acpd-13-23817-2013, 2013.
- Lewandowski, M., Piletic, I. R., Kleindienst, T. E., Offenberg, J. H., Beaver, M. R., Jaoui, M., Docherty, K. S., and Edney, E. O.: Secondary organic aerosol characterisation at field sites across the United States during the spring-summer period, *Int. J. Environ. An. Ch.*, 93, 1084–1103, doi:10.1080/03067319.2013.803545, 2013.
- Lewis, C. W., Klouda, G. A., and Ellenson, W. D.: Radiocarbon measurement of the biogenic contribution to summertime PM_{2.5} ambient aerosol in Nashville, TN, *Atmos. Environ.*, 38, 6053–6061, doi:10.1016/j.atmosenv.2004.06.011, 2004.
- 25 Lezberg, A. L., Battaglia, M. A., Shepperd, W. D., and Schoettle, A. W.: Decades-old silvicultural treatments influence surface wildfire severity and post-fire nitrogen availability in a ponderosa pine forest, *Forest Ecol. Manag.*, 255, 49–61, doi:10.1016/j.foreco.2007.08.019, 2008.
- Linkhart, B. D. and Reynolds, R. T.: Lifetime reproduction of Flammulated Owls in Colorado, *J. Raptor Res.*, 40, 29–37, doi:10.3356/0892-1016(2006)40[29:lrofoi]2.0.co;2, 2006.
- 30 Linkhart, B. D. and Reynolds, R. T.: Return rate, fidelity, and dispersal in a breeding population of flammulated owls (*Otus flammeolus*), *Auk*, 124, 264–275, doi:10.1642/0004-8038(2007)124[264:rrfadi]2.0.co;2, 2007.

Overview of the Manitou Experimental Forest Observatory

J. Ortega et al.

Title Page

Abstract

Introduction

Conclusions

References

Tables

Figures

⏪

⏩

◀

▶

Back

Close

Full Screen / Esc

Printer-friendly Version

Interactive Discussion

- Mahowald, N., Ward, D. S., Kloster, S., Flanner, M. G., Heald, C. L., Heavens, N. G., Hess, P. G., Lamarque, J. F., and Chuang, P. Y.: Aerosol impacts on climate and biogeochemistry, *Annu. Rev. Env. Resour.*, 36, 45–74, doi:10.1146/annurev-environ-042009-094507, 2011.
- Mao, J., Ren, X., Zhang, L., Van Duin, D. M., Cohen, R. C., Park, J.-H., Goldstein, A. H., Paulot, F., Beaver, M. R., Crounse, J. D., Wennberg, P. O., DiGangi, J. P., Henry, S. B., Keutsch, F. N., Park, C., Schade, G. W., Wolfe, G. M., Thornton, J. A., and Brune, W. H.: Insights into hydroxyl measurements and atmospheric oxidation in a California forest, *Atmos. Chem. Phys.*, 12, 8009–8020, doi:10.5194/acp-12-8009-2012, 2012.
- Massman, W. J., Frank, J. M., and Mooney, S. J.: Advancing investigation and physical modeling of first-order fire effects on soils, *Fire Ecology*, 6, 36–54, doi:10.4996/fireecology.0601036, 2010.
- Matsui, H., Koike, M., Kondo, Y., Takegawa, N., Wiedensohler, A., Fast, J. D., and Zaveri, R. A.: Impact of new particle formation on the concentrations of aerosols and cloud condensation nuclei around Beijing, *J. Geophys. Res.-Atmos.*, 116, 19, doi:10.1029/2011jd016025, 2011.
- Mirme, S., Mirme, A., Minikin, A., Petzold, A., Hörrak, U., Kerminen, V. -M., and Kulmala, M.: Atmospheric sub-3 nm particles at high altitudes, *Atmos. Chem. Phys.*, 10, 437–451, doi:10.5194/acp-10-437-2010, 2010.
- Morris, C. E., Conen, F., Huffman, J. A., Phillips, V., Pöschl, U., and Sands, D. C.: Bio-precipitation: a feedback cycle linking Earth history, ecosystem dynamics and land use through biological ice nucleators in the atmosphere, *Glob. Change Biol.*, 20, 341–351, doi:10.1111/gcb.12447, 2014.
- Moteki, N., Kondo, Y., and Nakamura, S.: Method to measure refractive indices of small non-spherical particles: application to black carbon particles, *J. Aerosol. Sci.*, 41, 513–521, 2010.
- Orlando, J. J. and Tyndall, G. S.: Laboratory studies of organic peroxy radical chemistry: an overview with emphasis on recent issues of atmospheric significance, *Chem. Soc. Rev.*, 41, 8213–8213, 2012.
- Ortega, A. M., Day, D. A., Cubison, M. J., Brune, W. H., Bon, D., de Gouw, J. A., and Jimenez, J. L.: Secondary organic aerosol formation and primary organic aerosol oxidation from biomass-burning smoke in a flow reactor during FLAME-3, *Atmos. Chem. Phys.*, 13, 11551–11571, doi:10.5194/acp-13-11551-2013, 2013.
- Paasonen, P., Asmi, A., Petaja, T., Kajos, M. K., Aijala, M., Junninen, H., Holst, T., Abbatt, J. P. D., Arneth, A., Birmili, W., van der Gon, H. D., Hamed, A., Hoffer, A., Laakso, L., Laaksonen, A., Leaitch, W. R., Plass-Dulmer, C., Pryor, S. C., Raisanen, P., Swietlicki, E.,

Overview of the Manitou Experimental Forest Observatory

J. Ortega et al.

Title Page

Abstract

Introduction

Conclusions

References

Tables

Figures

⏪

⏩

◀

▶

Back

Close

Full Screen / Esc

Printer-friendly Version

Interactive Discussion

Wiedensohler, A., Worsnop, D. R., Kerminen, V. M., and Kulmala, M.: Warming-induced increase in aerosol number concentration likely to moderate climate change, *Nat. Geosci.*, 6, 438–442, doi:10.1038/ngeo1800, 2013.

Peeters, J., Nguyen, T. L., and Vereecken, L.: HO_x radical regeneration in the oxidation of isoprene, *Phys. Chem. Chem. Phys.*, 11, 5935–5939, doi:10.1039/b908511d, 2009.

Petters, M. D. and Kreidenweis, S. M.: A single parameter representation of hygroscopic growth and cloud condensation nucleus activity, *Atmos. Chem. Phys.*, 7, 1961–1971, doi:10.5194/acp-7-1961-2007, 2007.

Pöhlker, C., Wiedemann, K. T., Sinha, B., Shiraiwa, M., Gunthe, S. S., Smith, M., Su, H., Artaxo, P., Chen, Q., Cheng, Y. F., Elbert, W., Gilles, M. K., Kilcoyne, A. L. D., Moffet, R. C., Weigand, M., Martin, S. T., Poeschl, U., and Andreae, M. O.: Biogenic potassium salt particles as seeds for secondary organic aerosol in the Amazon, *Science*, 337, 1075–1078, doi:10.1126/science.1223264, 2012.

Pöschl, U., Martin, S. T., Sinha, B., Chen, Q., Gunthe, S. S., Huffman, J. A., Borrmann, S., Farmer, D. K., Garland, R. M., Helas, G., Jimenez, J. L., King, S. M., Manzi, A., Mikhailov, E., Pauliquevis, T., Petters, M. D., Prenni, A. J., Roldin, P., Rose, D., Schneider, J., Su, H., Zorn, S. R., Artaxo, P., and Andreae, M. O.: Rainforest aerosols as biogenic nuclei of clouds and precipitation in the Amazon, *Science*, 329, 1513–1516, doi:10.1126/science.1191056, 2010.

Prenni, A. J., Tobo, Y., Garcia, E., DeMott, P. J., Huffman, J. A., McCluskey, C. S., Kreidenweis, S. M., Prenni, J. E., Pöhlker, C., and Pöschl, U.: The impact of rain on ice nuclei populations at a forested site in Colorado, *Geophys. Res. Lett.*, 40, 227–231, doi:10.1029/2012gl053953, 2013.

Pryor, S. C., Spaulding, A. M., and Barthelme, R. J.: New particle formation in the Midwestern USA: event characteristics, meteorological context and vertical profiles, *Atmos. Environ.*, 44, 4413–4425, doi:10.1016/j.atmosenv.2010.07.045, 2010.

Pryor, S. C., Barthelme, R. J., and Hornsby, K. E.: Size-resolved particle fluxes and vertical gradients over and in a sparse pine forest, *Aerosol Sci. Tech.*, 47, 1248–1257, 2013.

Rhoades, C. C., Battaglia, M. A., Rocca, M. E., and Ryan, M. G.: Short- and medium-term effects of fuel reduction mulch treatments on soil nitrogen availability in Colorado conifer forests, *Forest Ecol. Manag.*, 276, 231–238, doi:10.1016/j.foreco.2012.03.028, 2012.

Overview of the Manitou Experimental Forest Observatory

J. Ortega et al.

Title Page

Abstract

Introduction

Conclusions

References

Tables

Figures

◀

▶

◀

▶

Back

Close

Full Screen / Esc

Printer-friendly Version

Interactive Discussion

- Robinson, N. H., Allan, J. D., Huffman, J. A., Kaye, P. H., Foot, V. E., and Gallagher, M.: Cluster analysis of WIBS single-particle bioaerosol data, *Atmos. Meas. Tech.*, 6, 337–347, doi:10.5194/amt-6-337-2013, 2013.
- Rogers, D. C., DeMott, P. J., Kreidenweis, S. M., and Chen, Y. L.: A continuous-flow diffusion chamber for airborne measurements of ice nuclei, *J. Atmos. Ocean. Tech.*, 18, 725–741, doi:10.1175/1520-0426(2001)018<0725:acfdcf>2.0.co;2, 2001.
- Rollins, A. W., Smith, J. D., Wilson, K. R., and Cohen, R. C.: Real time in situ detection of organic nitrates in atmospheric aerosols, *Environ. Sci. Technol.*, 44, 5540–5545, doi:10.1021/es100926x, 2010.
- Sadanaga, Y., Yoshino, A., Watanabe, K., Yoshioka, A., Wakazono, Y., Kanaya, Y., and Kajii, Y.: Development of a measurement system of OH reactivity in the atmosphere by using a laser-induced pump and probe technique, *Rev. Sci. Instrum.*, 75, 2648–2655, doi:10.1063/1.1775311, 2004.
- Schobesberger, S., Vaananen, R., Leino, K., Virkkula, A., Backman, J., Pohja, T., Siivola, E., Franchin, A., Mikkilä, J., Paramonov, M., Aalto, P. P., Krejci, R., Petaja, T., and Kulmala, M.: Airborne measurements over the boreal forest of southern Finland during new particle formation events in 2009 and 2010, *Boreal Environ. Res.*, 18, 145–163, 2013.
- Schumacher, C. J., Pöhlker, C., Aalto, P., Hiltunen, V., Petäjä, T., Kulmala, M., Pöschl, U., and Huffman, J. A.: Seasonal cycles of fluorescent biological aerosol particles in boreal and semi-arid forests of Finland and Colorado, *Atmos. Chem. Phys.*, 13, 11987–12001, doi:10.5194/acp-13-11987-2013, 2013.
- Smith, J. N., Moore, K. F., McMurry, P. H., and Eisele, F. L.: Atmospheric measurements of sub-20 nm diameter particle chemical composition by thermal desorption chemical ionization mass spectrometry, *Aerosol Sci. Tech.*, 38, 100–110, doi:10.1080/02786820490249036, 2004.
- Stone, D., Whalley, L. K., and Heard, D. E.: Tropospheric OH and HO₂ radicals: field measurements and model comparisons, *Chem. Soc. Rev.*, 41, 6348–6404, doi:10.1039/c2cs35140d, 2012.
- Tanner, D. J., Jefferson, A., and Eisele, F. L.: Selected ion chemical ionization mass spectrometric measurement of OH, *J. Geophys. Res.-Atmos.*, 102, 6415–6425, doi:10.1029/96jd03919, 1997.
- Thornton, J. A., Wooldridge, P. J., Cohen, R. C., Martinez, M., Harder, H., Brune, W. H., Williams, E. J., Roberts, J. M., Fehsenfeld, F. C., Hall, S. R., Shetter, R. E., Wert, B. P.,

Overview of the Manitou Experimental Forest Observatory

J. Ortega et al.

Title Page

Abstract

Introduction

Conclusions

References

Tables

Figures

◀

▶

◀

▶

Back

Close

Full Screen / Esc

Printer-friendly Version

Interactive Discussion

and Fried, A.: Ozone production rates as a function of NO_x abundances and HO_x production rates in the Nashville urban plume, *J. Geophys. Res.*, 107, 4146–4163, doi:10.1029/2001JD000932, 2002.

5 Tobo, Y., Prenni, A. J., DeMott, P. J., Huffman, J. A., McCluskey, C. S., Tian, G., Pöhlker, C., Pöschl, U., Kreidenweis, S. M.: Biological aerosol particles as a key determinant of ice nuclei populations in a forest ecosystem, *J. Geophys. Res.-Atmos.*, 118, 10100–10110, doi:10.1002/jgrd.50801, 2013.

10 Vogel, A. L., Äijälä, M., Brüggemann, M., Ehn, M., Junninen, H., Petäjä, T., Worsnop, D. R., Kulmala, M., Williams, J., and Hoffmann, T.: Online atmospheric pressure chemical ionization ion trap mass spectrometry (APCI-IT- MS_n) for measuring organic acids in concentrated bulk aerosol – a laboratory and field study, *Atmos. Meas. Tech.*, 6, 431–443, doi:10.5194/amt-6-431-2013, 2013.

15 Vorosmarty, C. J., McIntyre, P. B., Gessner, M. O., Dudgeon, D., Prusevich, A., Green, P., Glidden, S., Bunn, S. E., Sullivan, C. A., Liermann, C. R., and Davies, P. M.: Global threats to human water security and river biodiversity, *Nature*, 467, 555–561, doi:10.1038/nature09440, 2010.

Wagner, N. L., Dubé, W. P., Washenfelder, R. A., Young, C. J., Pollack, I. B., Ryerson, T. B., and Brown, S. S.: Diode laser-based cavity ring-down instrument for NO_3 , N_2O_5 , NO , NO_2 and O_3 from aircraft, *Atmos. Meas. Tech.*, 4, 1227–1240, doi:10.5194/amt-4-1227-2011, 2011.

20 Wolfe, G. M., Thornton, J. A., Bouvier-Brown, N. C., Goldstein, A. H., Park, J.-H., McKay, M., Matross, D. M., Mao, J., Brune, W. H., LaFranchi, B. W., Browne, E. C., Min, K.-E., Wooldridge, P. J., Cohen, R. C., Crouse, J. D., Faloon, I. C., Gilman, J. B., Kuster, W. C., de Gouw, J. A., Huisman, A., and Keutsch, F. N.: The Chemistry of Atmosphere-Forest Exchange (CAFE) Model – Part 2: Application to BEARPEX-2007 observations, *Atmos. Chem. Phys.*, 11, 1269–1294, doi:10.5194/acp-11-1269-2011, 2011.

25 Wolfe, G. M., Cantrell, C., Kim, S., Mauldin III, R. L., Karl, T., Harley, P., Turnipseed, A., Zheng, W., Flocke, F., Apel, E. C., Hornbrook, R. S., Hall, S. R., Ullmann, K., Henry, S. B., DiGangi, J. P., Boyle, E. S., Kaser, L., Schnitzhofer, R., Hansel, A., Graus, M., Nakashima, Y., Kajii, Y., Guenther, A., and Keutsch, F. N.: Missing peroxy radical sources within a rural forest canopy, *Atmos. Chem. Phys. Discuss.*, 13, 31713–31759, doi:10.5194/acpd-13-31713-2013, 2013.

30 Yatavelli, R. L. N., Lopez-Hilfiker, F., Wargo, J. D., Kimmel, J. R., Cubison, M. J., Bertram, T. H., Jimenez, J. L., Gonin, M., Worsnop, D. R., and Thornton, J. A.: A Chemical Ionization High-Resolution Time-of-Flight Mass Spectrometer Coupled to a Micro Orifice Volatilization Im-

Overview of the Manitou Experimental Forest Observatory

J. Ortega et al.

Title Page

Abstract

Introduction

Conclusions

References

Tables

Figures

⏪

⏩

◀

▶

Back

Close

Full Screen / Esc

Printer-friendly Version

Interactive Discussion

pactor (MOVI-HRToF-CIMS) for analysis of gas and particle-phase organic species, *Aerosol Sci. Tech.*, 46, 1313–1327, doi:10.1080/02786826.2012.712236, 2012.

Yatavelli, R. L. N., Stark, H., Thompson, S. L., Kimmel, J. R., Cubison, M. J., Day, D. A., Campuzano-Jost, P., Palm, B. B., Thornton, J. A., Jayne, J. T., Worsnop, D. R., and Jimenez, J. L.: Semi-continuous measurements of gas/particle partitioning of organic acids in a ponderosa pine forest using a MOVI-HRToF-CIMS, *Atmos. Chem. Phys. Discuss.*, 13, 17327–17374, doi:10.5194/acpd-13-17327-2013, 2013.

Zhang, H. F., Worton, D. R., Lewandowski, M., Ortega, J., Rubitschun, C. L., Park, J. H., Kristensen, K., Campuzano-Jost, P., Day, D. A., Jimenez, J. L., Jaoui, M., Offenber, J. H., Kleindienst, T. E., Gilman, J., Kuster, W. C., de Gouw, J., Park, C., Schade, G. W., Frossard, A. A., Russell, L., Kaser, L., Jud, W., Hansel, A., Cappellin, L., Karl, T., Glasius, M., Guenther, A., Goldstein, A. H., Seinfeld, J. H., Gold, A., Kamens, R. M., and Surratt, J. D.: Organosulfates as tracers for Secondary Organic Aerosol (SOA) formation from 2-methyl-3-buten-2-ol (MBO) in the Atmosphere, *Environ. Sci. Technol.*, 46, 9437–9446, doi:10.1021/es301648z, 2012.

Zhao, J., Eisele, F. L., Titcombe, M., Kuang, C. G., and McMurry, P. H.: Chemical ionization mass spectrometric measurements of atmospheric neutral clusters using the cluster-CIMS, *J. Geophys. Res.-Atmos.*, 115, 19, doi:10.1029/2009jd012606, 2010.

Zhao, J., Smith, J. N., Eisele, F. L., Chen, M., Kuang, C., and McMurry, P. H.: Observation of neutral sulfuric acid-amine containing clusters in laboratory and ambient measurements, *Atmos. Chem. Phys.*, 11, 10823–10836, doi:10.5194/acp-11-10823-2011, 2011.

Zhao, Y. L., Kreisberg, N. M., Worton, D. R., Teng, A. P., Hering, S. V., and Goldstein, A. H.: Development of an in situ thermal desorption gas chromatography instrument for quantifying atmospheric semi-volatile organic compounds, *Aerosol Sci. Tech.*, 47, 258–266, doi:10.1080/02786826.2012.747673, 2013.

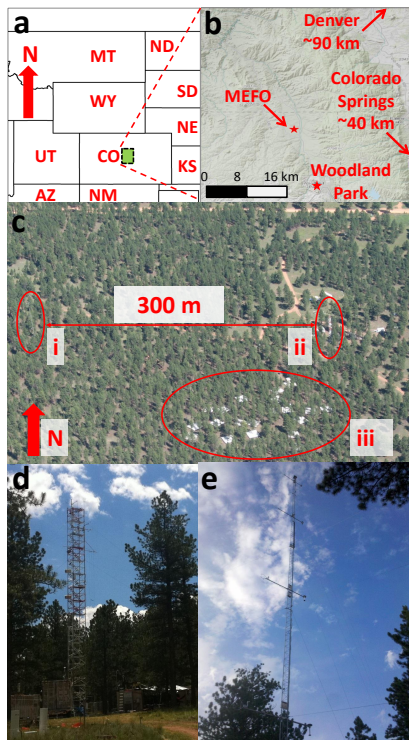


Fig. 1. Manitou Experimental Forest Observatory (MEFO). **(a)** Map showing general area within Colorado and its relationship to neighboring states. **(b)** Site location relative to the Front Range urban corridor including Denver and Colorado Springs. **(c)** Close-up aerial photograph showing the open-canopy ponderosa pine-dominated forest with the (i) micrometeorological tower, (ii) chemistry tower, and (iii) water manipulation experiment. **(d)** Close up picture of Chemistry tower. **(e)** Close of up picture of micrometeorological tower. The two towers shown in **(c)** are approximately 300 m apart. Maps in panels **(a)** and **(b)** were produced using ArcGIS software (ESRI Inc., Redlands, CA).

Overview of the Manitou Experimental Forest Observatory

J. Ortega et al.

Title Page

Abstract

Introduction

Conclusions

References

Tables

Figures

◀

▶

◀

▶

Back

Close

Full Screen / Esc

Printer-friendly Version

Interactive Discussion

Overview of the Manitou Experimental Forest Observatory

J. Ortega et al.

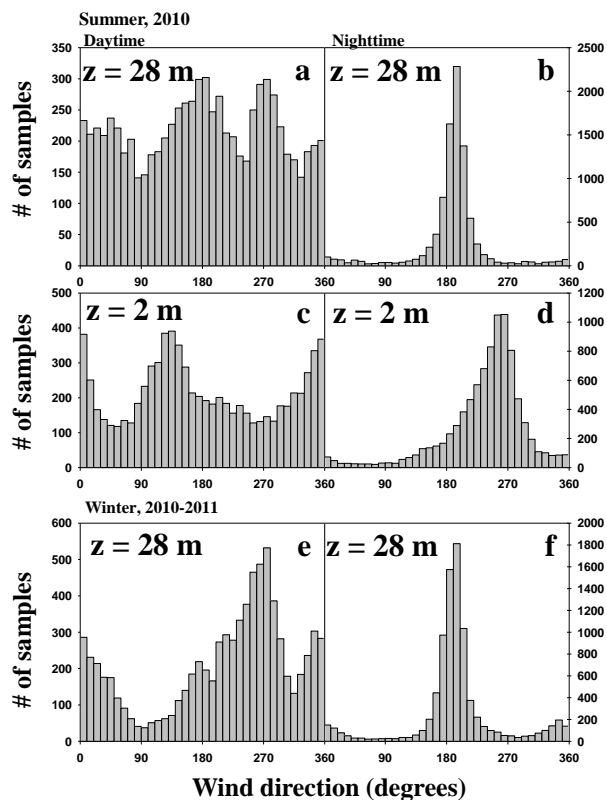


Fig. 2. Wind direction distributions (5 min averages binned every 10°) from the MEFO Chemistry tower. Panels (a), (c) and (e) are daytime wind distributions (9:00–17:00 MST) whereas panels (b), (d) and (f) are for nighttime hours (20:00 until 5:00 MST). Summer includes data from June–August 2010. Winter includes data from December 2010 to February 2011. Measurement height is noted on the panels.

[Title Page](#)
[Abstract](#)
[Introduction](#)
[Conclusions](#)
[References](#)
[Tables](#)
[Figures](#)
[⏪](#)
[⏩](#)
[◀](#)
[▶](#)
[Back](#)
[Close](#)
[Full Screen / Esc](#)
[Printer-friendly Version](#)
[Interactive Discussion](#)

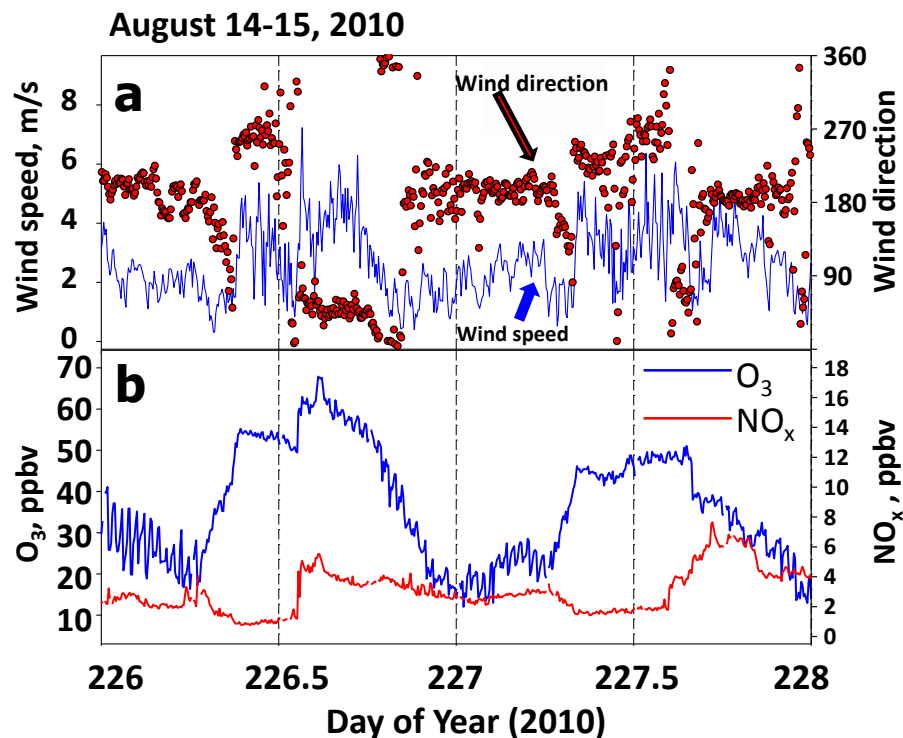


Fig. 3. Time series of wind speed, wind direction, ozone and NO_x as measured from the MEFO chemistry tower (14–15 August 2010) showing typical summertime patterns. Meteorological variables were measured at the top of the tower (25.1 m) and the trace gases were measured using the 6 point gradient system (Table S1). Ozone deposition and resulting gradients lead to the nighttime variability. In contrast, NO_x is nearly constant through the canopy, implying negligible soil emissions.

Overview of the Manitou Experimental Forest Observatory

J. Ortega et al.

Title Page

Abstract

Introduction

Conclusions

References

Tables

Figures

◀

▶

◀

▶

Back

Close

Full Screen / Esc

Printer-friendly Version

Interactive Discussion

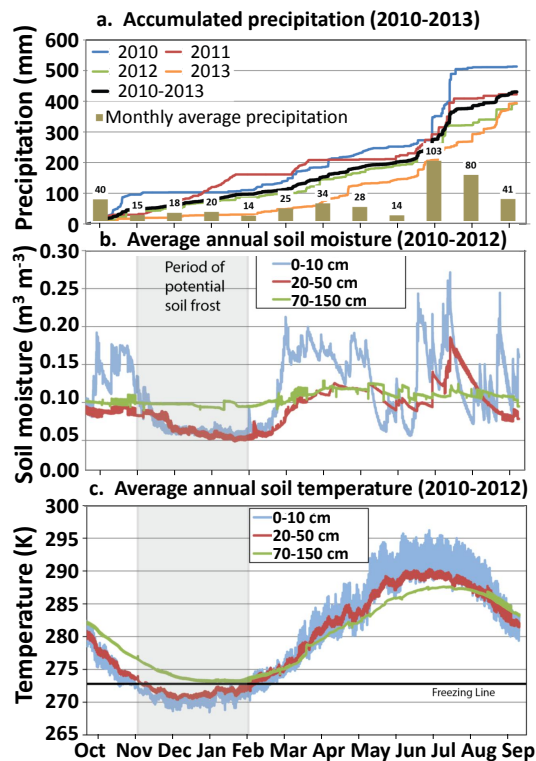


Fig. 4. Hydrological measurement summary at the Manitou Experimental Forest Observatory. Annual accumulated precipitation from rain and snow **(a)**, soil moisture at 3 depths **(b)**, and soil temperature at three different depths **(c)**. Note that the hydrological year is defined from as ending on 30 September with a start date of 1 October of the preceding year. Panel **(a)** includes data from hydrological years 2010–2013 whereas panels **(b)** and **(c)** include data from 2010–2012.

Overview of the Manitou Experimental Forest Observatory

J. Ortega et al.

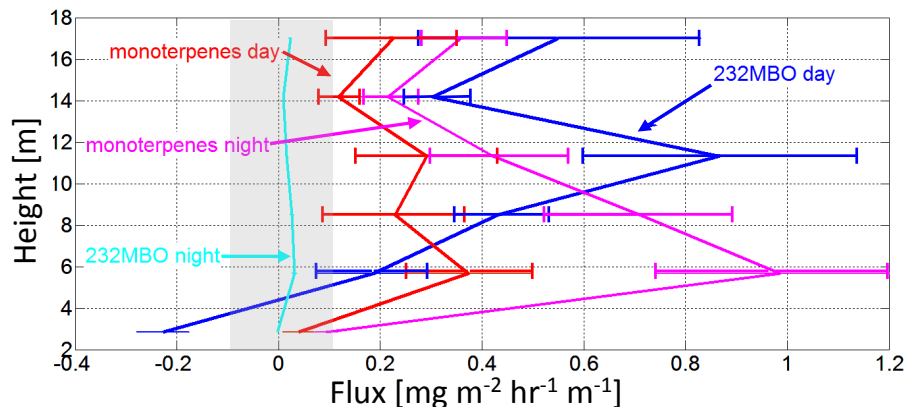


Fig. 5. Average daytime and nighttime vertical fluxes of monoterpenes ($C_{10}H_{16}$) and 2-methyl-3-buten-2-ol (232MBO, $C_5H_{10}O$) during August 2010. The average daytime integrated flux ratio of MBO : Monoterpenes is 1.65. Fluxes within $\pm 0.1 \text{ mg m}^{-2} \text{ h}^{-1} \text{ m}^{-1}$ are shown within the shaded grey area to indicate the detection limit. Error bars indicate the standard deviation of all measurements for that chemical species and level.

Title Page

Abstract

Introduction

Conclusions

References

Tables

Figures

◀

▶

◀

▶

Back

Close

Full Screen / Esc

Printer-friendly Version

Interactive Discussion

Overview of the Manitou Experimental Forest Observatory

J. Ortega et al.

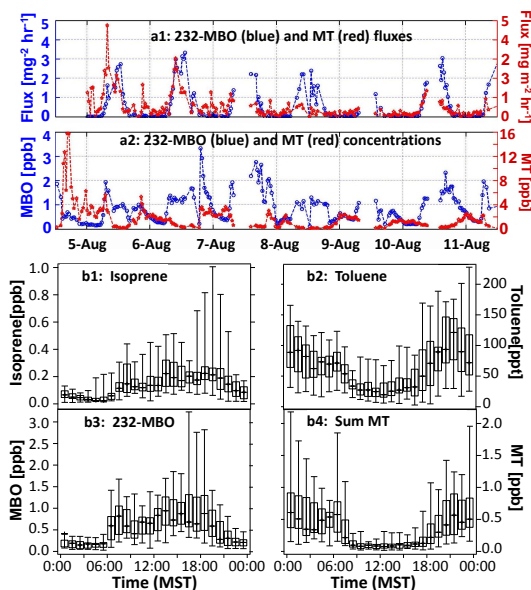


Fig. 6. (a) (adapted from Kaser et al., 2013b) shows the sum of MT and MBO + isoprene measurements as reported by the PTR-TOF-MS from 25.1 m on the chemistry tower from 4 August (DOY = 216) to 11 August 2010 (DOY = 223). Top panel (**a-1**) shows the above-canopy fluxes, while (**a-2**) shows the corresponding concentrations in ppbv. An intense hailstorm on the afternoon of 4 August 2010 (doy = 216) caused the anomalously high MT concentrations and fluxes that lasted for ~ 2 days after the event. This effect is due to mechanical disturbance, which released MT stored in pools within the needle structures. MBO, which is produced during photosynthesis and immediately emitted, was not noticeably affected by the event. Bottom panel (**b**) shows diurnal profiles of (**b-1**) isoprene, (**b-2**) toluene, (**b-3**) MBO, and (**b-4**) sum of monoterpenes during all of August 2010 as measured using TOGA. Box boundaries indicate inter-quartile range, median is indicated as the line through the box, and whisker lengths indicate the total measurement range.

[Title Page](#)
[Abstract](#)
[Introduction](#)
[Conclusions](#)
[References](#)
[Tables](#)
[Figures](#)
[◀](#)
[▶](#)
[◀](#)
[▶](#)
[Back](#)
[Close](#)
[Full Screen / Esc](#)
[Printer-friendly Version](#)
[Interactive Discussion](#)

Overview of the
Manitou
Experimental Forest
Observatory

J. Ortega et al.

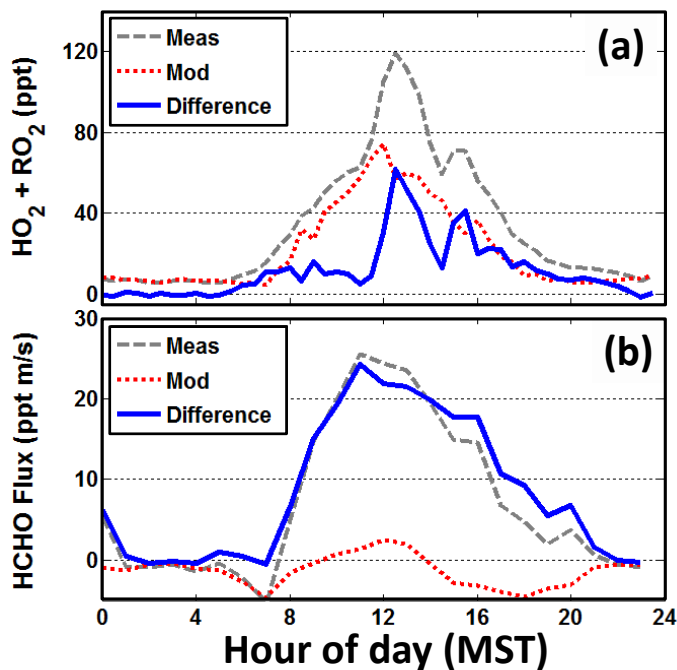


Fig. 7. Average modeled and measured diurnal cycles of **(a)** within-canopy peroxy radical mixing ratios, and **(b)** above-canopy formaldehyde fluxes. The measured and modeled results for both compounds include the hourly averages from the August 2010 BEACHON ROCS intensive measurement campaign. Model calculations of HCHO fluxes and peroxy radicals are described in DiGangi et al. (2011) and Wolfe et al. (2013), respectively.

[Title Page](#)[Abstract](#)[Introduction](#)[Conclusions](#)[References](#)[Tables](#)[Figures](#)[⏪](#)[⏩](#)[◀](#)[▶](#)[Back](#)[Close](#)[Full Screen / Esc](#)[Printer-friendly Version](#)[Interactive Discussion](#)

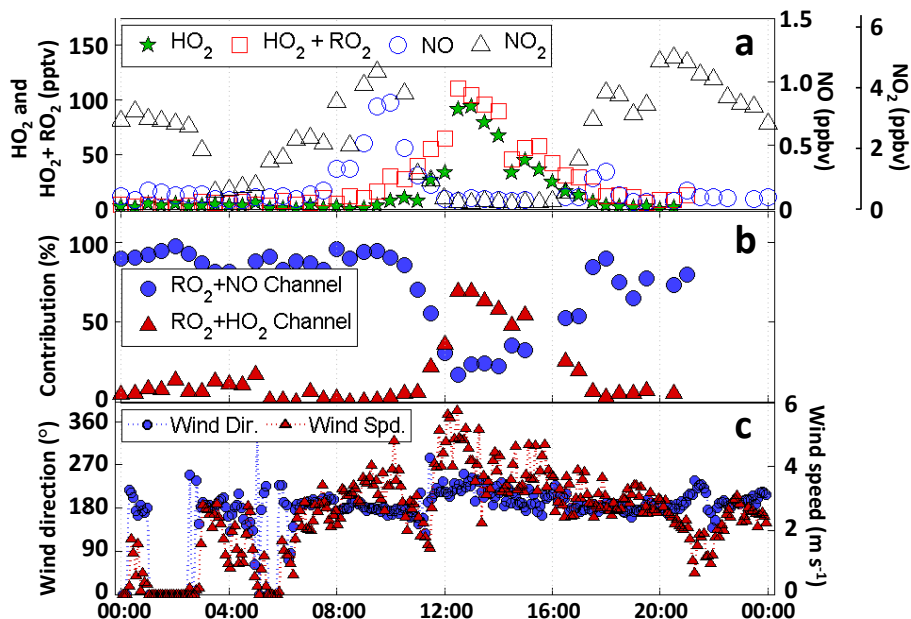


Fig. 8. Examination of RO_2 fate and its relation to anthropogenic influence on 24 August 2010 during BEACHON-ROCS. The first panel (a) shows median concentrations of NO , NO_2 , HO_2 , and $\text{HO}_2 + \text{RO}_2$ over the course of this day. Wind speed and direction (c) show the wind shifting from out of the south to out of the southeast just prior to noon indicating an anthropogenic influence from the Colorado Springs area. This transition is also reflected in the NO increase in panel (a). The middle panel (b) shows the calculated RO_2 loss percentage from reaction with NO or HO_2 based on measured NO and HO_2 concentrations and on rate constants obtained from the IUPAC database. Each symbol in (b) represents the median value from thirty minute time bins. Figure adapted from DiGangi et al. (2012).

Overview of the Manitou Experimental Forest Observatory

J. Ortega et al.

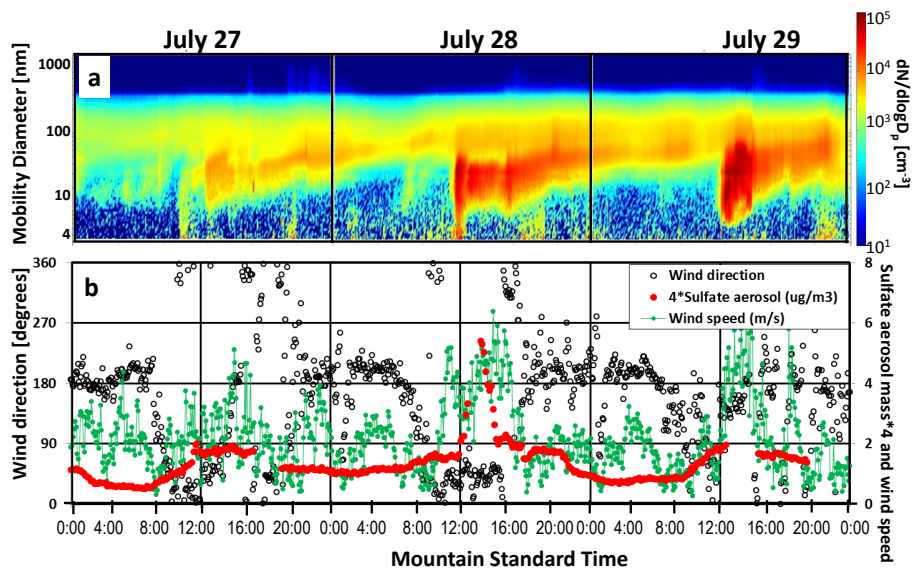


Fig. 9. Three representative days of particle size distributions (a), wind speed, wind direction and sulfate aerosol mass (b) during 27–29 July 2011. In panel (a), the mobility diameter is on the y axis, time is on the x axis, and the color bar indicates particle number concentration ($dN/d\log D_p$) in cm^{-3} . In panel (b), the sulfate aerosol mass is multiplied by 4 and is listed on the 2nd y axis along with wind speed.

Title Page

Abstract

Introduction

Conclusions

References

Tables

Figures

◀

▶

◀

▶

Back

Close

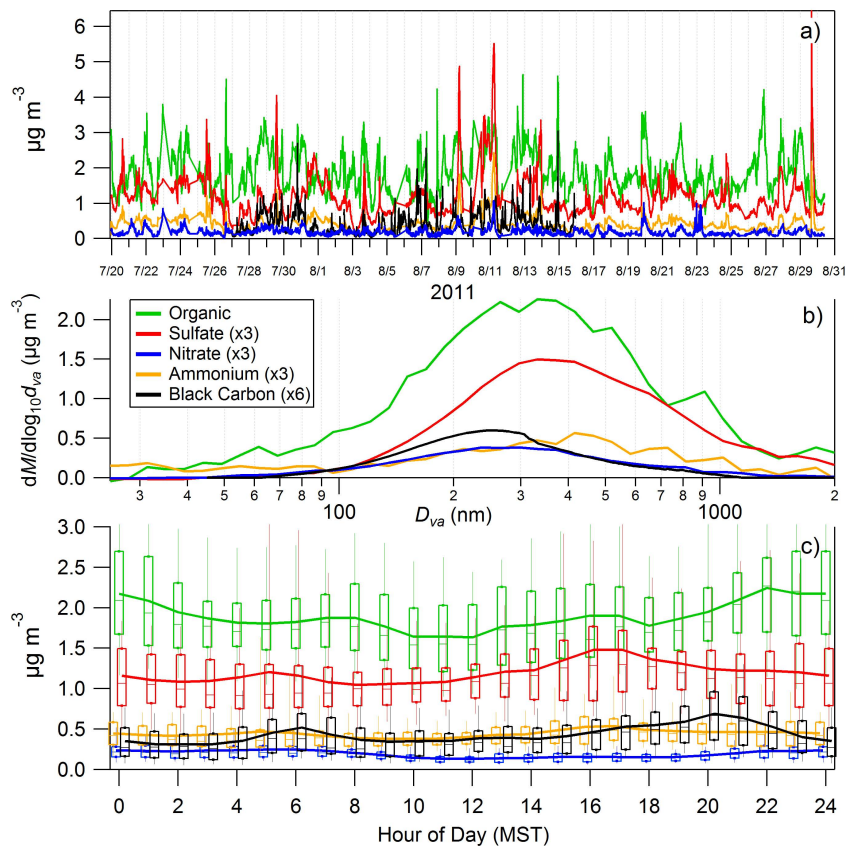
Full Screen / Esc

Printer-friendly Version

Interactive Discussion

**Overview of the
Manitou
Experimental Forest
Observatory**

J. Ortega et al.



Title Page

Abstract Introduction

Conclusions References

Tables Figures

⏪ ⏩

⏴ ⏵

Back Close

Full Screen / Esc

Printer-friendly Version

Interactive Discussion



Overview of the Manitou Experimental Forest Observatory

J. Ortega et al.

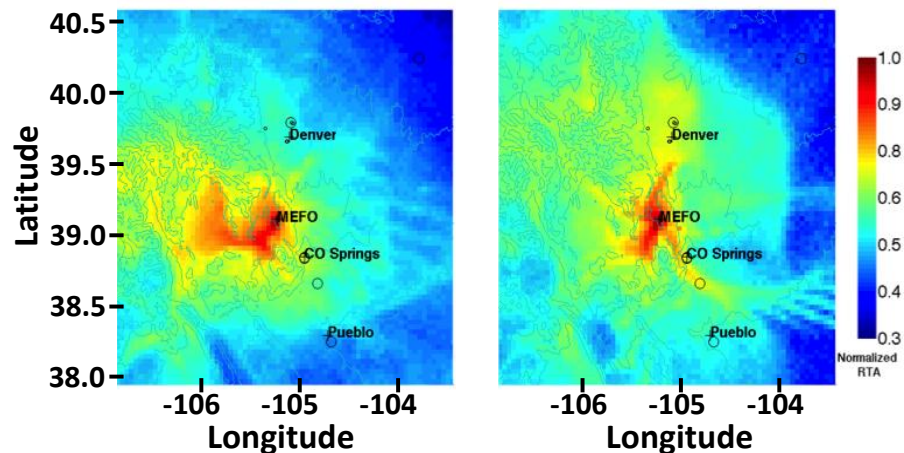


Fig. 11. Residence Time Analysis (RTA) from WRF-Chem estimates the amount of time that air masses originate from the various locations in the region. These simulations estimate 48 hour back-trajectories at MEFO (27 July to 26 August 2011). Three major Front Range cities (Denver, Colorado Springs, and Pueblo), are shown, and open circles indicate the cities' primary coal-fired power plants. The left panel indicates that the majority of the low NO_2 concentration results (0–50th percentile) are from air masses that originate from the west. The right panel shows that the highest 10 % of NO_2 concentrations originate from the Front Range cities and are advected to the site.

Overview of the Manitou Experimental Forest Observatory

J. Ortega et al.

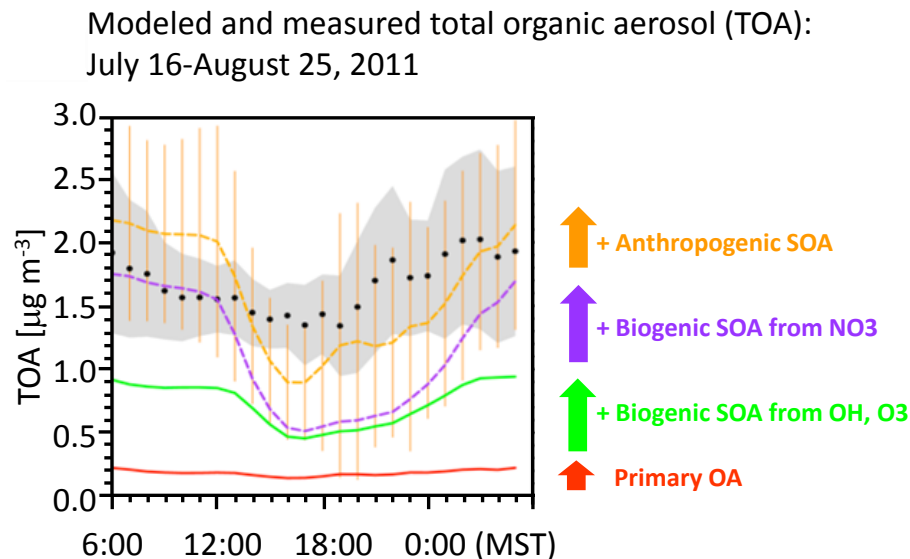


Fig. 12. Modeled and measured average diurnal profiles of total organic aerosol (TOA) mass concentrations at MEFO during BEACHON-RoMBAS-2011. Aerosol mass spectrometry (AMS) observations are shown as black circles (with 1σ variability shown in gray). Predicted TOA is indicated in yellow (with variability shown by the yellow bars). The predicted TOA is the sum of the contributions: primary OA (red), biogenic secondary organic aerosol (SOA) from OH and O_3 chemistry (green), biogenic SOA from NO_3 nighttime chemistry (purple) and anthropogenic SOA (yellow). Each plot (starting with green) is additive (equal to that process plus the sum of the processes below it): e.g. the purple plot shows the contributions from primary OA, biogenic SOA from OH and O_3 and biogenic SOA + NO_3 . Biogenic SOA (both day and night) are the largest contributors to TOA, but anthropogenic species (gold) also make a significant contribution.

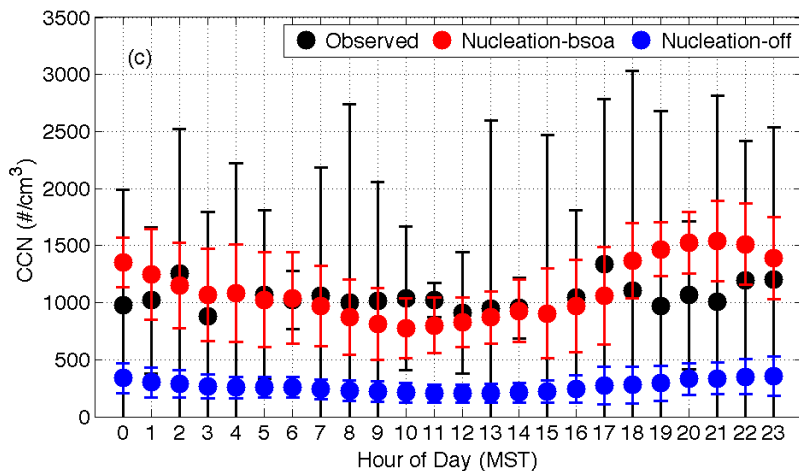
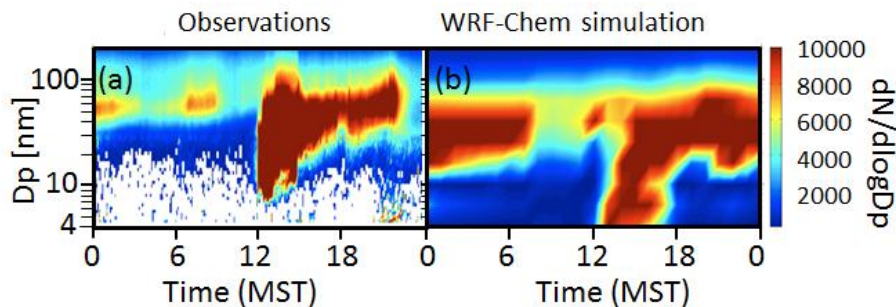


Fig. 13. 29 July 2011 particle size distributions observed **(a)** and modeled with WRF-Chem **(b)**. White areas in panel **(a)** indicate that no counts were observed for that diameter particle at that time. Panel **(c)** shows the observed (black) and predicted (red) CCN concentrations averaged over the 10–15 August 2011 time period. The blue circles are the simulations when nucleation is not included, which demonstrates the importance of particle nucleation for CCN formation.

Title Page	
Abstract	Introduction
Conclusions	References
Tables	Figures
◀	▶
◀	▶
Back	Close
Full Screen / Esc	
Printer-friendly Version	
Interactive Discussion	